# Boryl−Metal Bonds Facilitate Cobalt/Nickel-Catalyzed Olefin Hydrogenation

Tzu-Pin Lin and Jonas C. Peters*

Division of Chemistry and Chemical Engineering, California Institute of Technology, Pasadena, California 91125, United States

 ⓢ Supporting Information

ABSTRACT: New approaches toward the generation of late first-row metal catalysts that efficiently facilitate two-electron reductive transformations (e.g., hydrogenation) more typical of noble-metal catalysts is an important goal. Herein we describe the synthesis of a structurally unusual $S = 1$ bimetallic Co complex, $[(^{Cy}PBP)CoH]_2$ (**1**), supported by bis(phosphino)boryl and bis(phosphino)hydridoborane ligands. This complex reacts reversibly with a second equivalent of H_2 (1 atm) and serves as an olefin hydrogenation catalyst under mild conditions (room temperature, 1 atm H_2). A bimetallic Co species is invoked in the rate-determining step of the catalysis according to kinetic studies. A structurally related $Ni^I Ni^I$ dimer, $[(^{Ph}PBP)Ni]_2$ (**3**), has also been prepared. Like Co catalyst **1**, Ni complex **3** displays reversible reactivity toward H_2, affording the bimetallic complex $[(^{Ph}PBHP)NiH]_2$ (**4**). This reversible behavior is unprecedented for Ni^I species and is attributed to the presence of a boryl−Ni bond. Lastly, a series of monomeric $(^{tBu}PBP)NiX$ complexes (X = Cl (**5**), OTf (**6**), H (**7**), OC(H)O (**8**)) have been prepared. The complex $(^{tBu}PBP)NiH$ (**7**) shows enhanced catalytic olefin hydrogenation activity when directly compared with its isoelectronic/isostructural analogues where the boryl unit is substituted by a phenyl or amine donor, a phenomenon that we posit is related to the strong trans influence exerted by the boryl ligand.
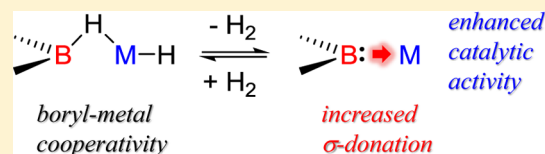
INTRODUCTION

Catalytic hydrogenation of unsaturated hydrocarbons constitutes one of the most broadly used methods in the production of valuable chemicals.[1] While these reactions are often catalyzed by precious metals, a growing interest in the use of earth-abundant first-row metals has emerged.[2] Substituting precious-metal catalysts with inexpensive base metals can be hampered by the inherent tendency of 3d metals to undergo one-electron reactions, thus bypassing desired two-electron processes such as oxidative addition or reductive elimination.[3] Reflecting this challenge is the limited number of Co[4] and Ni[4f,5] homogeneous olefin hydrogenation catalysts reported to date. Independent studies from Budzelaar[4a] and Chirik[4b] have shown catalytic olefin hydrogenations by pyridyl diimine Co complexes $(^{Ar}PDI)CoR$ (Chart 1). These results have highlighted the role of redox-active ligands in multielectron catalysis.[6] Hanson recently reported Co[4c,g] and Ni[5c] catalysts supported by bis(phosphino)amido (^{Cy}PNP) and bis-(phosphino)amino $(^{Cy}PNHP)$ ligands, respectively. Tetrametallic Co and Ni complexes $[(^{tBu}PN)M]_4$ (M = Co, Ni) have been described by Stryker in the context of alkene hydrogenation.[4f] As part of our ongoing interest in this field,[7] we recently reported the bis(phosphino)borane−Ni catalyst $(^{Ph}DPB)Ni$[5e] and the bis(phosphino)boryl−Co catalyst $(^{tBu}PBP)Co(N_2)$.[4d] Illustrating ligand−metal cooperativity in small-molecule activation,[8] both the borane−Ni and boryl−Co subunits appear to cooperatively[9] activate H_2 via a net two-electron process.[10]

Historically, boryl−metal complexes have been extensively studied because of their relevance in catalytic borylation

Chart 1. Several Recent Examples of Co and Ni Olefin Hydrogenation Catalysts
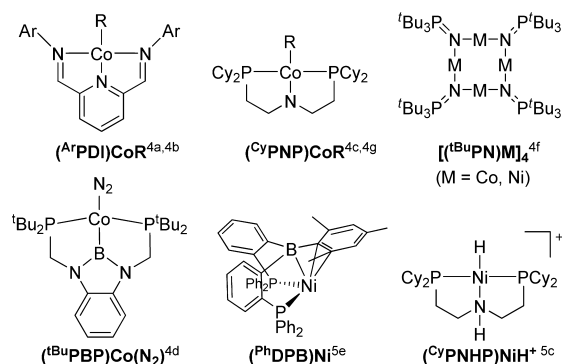
reactions.[11] Well-recognized for their strong trans influence, boryl ligands have been shown to significantly alter the electronic structure of transition metals.[12] Nevertheless, the utility of boryl functionalities has yet to be evaluated in the context of many prototypical catalytic transformations.[13] To further understand the role of boryl ligands in catalytic hydrogenation reactions, we herein describe the synthesis of a series of boryl−Co/Ni complexes, some of which display unusual reversible reactions with H_2 through ligand−metal cooperativity. Spectroscopic and kinetic data provide insight into the mechanisms of catalytic olefin hydrogenation by these

complexes. An efficient hydrogenation rate by one of the boryl−Ni catalysts is highlighted by direct comparison with its isoelectronic phenyl and amino congeners.

■ RESULTS AND DISCUSSION

Synthesis of Bimetallic Boryl−Co Complexes. Reaction of the ^{Cy}PB(H)P ligand, whose synthesis was provided by Yamashita and Nozaki,[14] with CoI_2 and sodium amalgam in tetrahydrofuran (THF) afforded the bimetallic complex $[(^{Cy}PBP)CoH]_2$ (1) in good yield (Scheme 1). Single-crystal

Scheme 1. Synthesis of Complexes 1 and [2][PF$_6$]
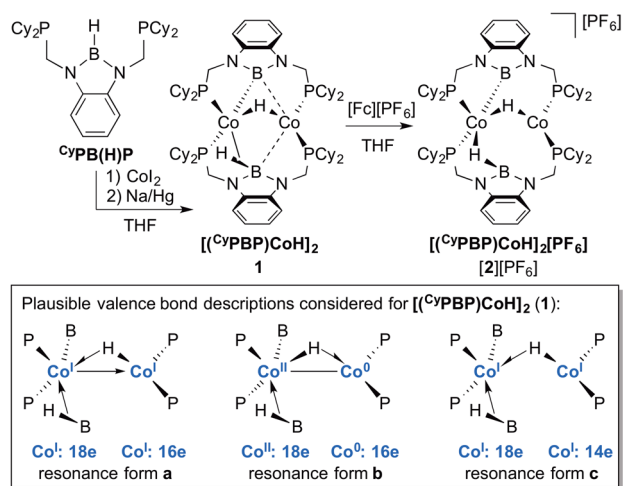
X-ray diffraction analysis reveals two Co centers with distinct coordination environments (Figure 1). The Co1 center is

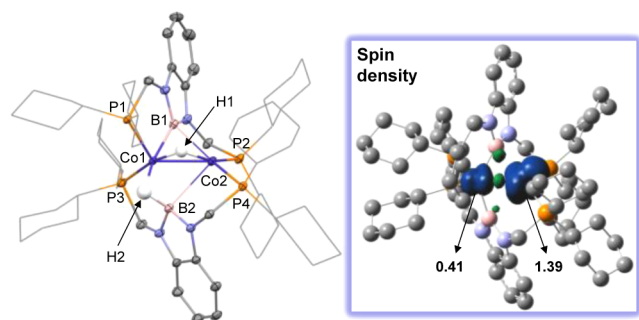**Figure 1.** (left) Solid-state structure of $[(^{Cy}PBP)CoH]_2$ (1). Thermal ellipsoids are drawn at the 50% probability level. Cyclohexyl groups are drawn in wireframe. Solvent molecules and hydrogen atoms (except for the bridging hydrides) have been omitted for clarity. Pertinent metrical parameters can be found in Table 1. (right) Mulliken atomic spin density surface of 1 (isovalue = 0.003). Hydrogen atoms have been omitted for clarity.

ligated by a boryl ligand (Co1−B1 2.049(2) Å) and an η^2-hydridoborane ligand (Co1−B2 2.006(2) Å).[15] In addition, the binuclear cobalt core is bridged by a hydride (Co1−H1 1.51(2) Å, Co2−H1 1.65(2) Å). A short Co1−Co2 bond of 2.3542(3) Å is measured, consistent with those observed for Co dimers featuring bridging hydride ligands.[16] On the basis of the structure analysis, three Lewis representations out of numerous possibilities were considered as most plausible for complex 1 (Scheme 1). In resonance form a, the bridging hydride is covalently bound to Co2, resulting in a formally Co^{I}Co^I

complex. A mixed-valent Co^{II}Co^0 dimer is invoked according to resonance form **b**. When the two Co centers are connected with a dative bond (form **a**) or a covalent bond (form **b**), the same electron counts (18 electrons for Co1, 16 electrons for Co2) are attained according to the covalent bond classification (CBC) method.[17] Lastly, resonance form **c** depicts a bonding situation in which two Co^I atoms are linked by a bridging hydride with no direct Co−Co bond.

Complex 1 is paramagnetic with a solution magnetic moment of $\mu_{eff} = 2.81\mu_B$ ($S = 1$) as a dimer or $1.99\mu_B$ ($S = \frac{1}{2}$) as a monomer (298 K, C_6D_6, Evans method).[18] The lack of an observable electron paramagnetic resonance (EPR) signal of complex 1 at room temperature (RT) or 77 K in 2-Me-THF is consistent with an $S = 1$ spin state. The solution IR spectrum of complex 1 in C_6H_6 is essentially identical to the solid-state attenuated total reflectance (ATR) IR spectrum, as both display a broad B−H stretch at 1651 cm^{-1}. ^{1}H diffusion-ordered spectroscopy (DOSY) NMR experiments [see the Supporting Information (SI)] indicate that the diffusion coefficient of 1 in C_6D_6 is much smaller than that of the monomeric boryl−Ni complex (vide infra).[19] Taken collectively, these data indicate that complex 1 exists as a *dimer* in solution.

The spin density plot shown in Figure 1 provides further insight into the electronic structure of 1. The calculated spin densities on Co1 and Co2 are, respectively, 0.41 and 1.39, which is more consistent with a Co^{I}Co^I configuration (resonance forms **a** and **c**). To evaluate the bonding situation in the Co−(μ_2-H)−Co moiety, we performed a natural orbital (NO) analysis on a simplified model complex, $[(^{Me}PBP)CoH]_2$ (1′). This calculation indicated that no net Co−Co bond is present and that the two Co atoms are involved in a three-center two-electron interaction through the bridging hydride (resonance form **c**), reminiscent of that found in the Ni system (vide infra). The NO analysis also suggested that the two unpaired electrons are ferromagnetically aligned in two orthogonal π^*(Co−Co) orbitals, leading to an $S = 1$ spin state (see the SI).

The cyclic voltammogram trace acquired for 1 in THF shows that the first oxidation and reduction waves are reversible with $E_{1/2}$ values of −1.34 and −2.91 V vs ferrocene/ferrocenium (Fc/Fc$^+$), respectively (see the SI). Treatment of 1 with [Fc][PF$_6$] in THF afforded the one-electron-oxidized product $[(^{Cy}PBP)CoH]_2[PF_6]$ ([2][PF$_6$]) in moderate yield (Scheme 1). The ^{1}H NMR spectrum of [2][PF$_6$] displays 52 resolved resonances, indicating a highly unsymmetrical ground state (a total of 72 ^{1}H resonances are possible if all are resolved in the unsymmetrical molecule). The solution magnetic moment of $\mu_{eff} = 1.62\mu_B$ (298 K, THF-d_8) is consistent with an $S = \frac{1}{2}$ species. Accordingly, the EPR spectrum of [2][PF$_6$] at 77 K in 2-Me-THF exhibits a rhombic signal (g = [2.400, 2.210, 2.010]; Figure 2) showing anisotropic hyperfine coupling with one ^{59}Co ($I = \frac{7}{2}$, A = [50, 50, 170] MHz) and two ^{31}P ($I = \frac{1}{2}$, A = [330, 120, 50] MHz) nuclei. An essentially identical spectrum was obtained for $[(^{Cy}PBP)CoD]_2$ [PF$_6$] ([2][PF$_6$]-d_2) prepared from $[(^{Cy}PBP)CoD]_2$ (1-d_2). No ^{1}H hyperfine tensor could be resolved.

Slow diffusion of Et$_2$O into a THF solution of [2][PF$_6$] afforded brown crystals suitable for X-ray diffraction analysis (Figure 3). Complex [2][PF$_6$] crystallizes in space group $P\bar{1}$ with two independent yet nearly identical molecules in the asymmetric unit.[20] As in the case of 1, two bridging hydrides between Co1 and Co2 as well as between Co1 and B2 were located in the difference map. The most substantial structural
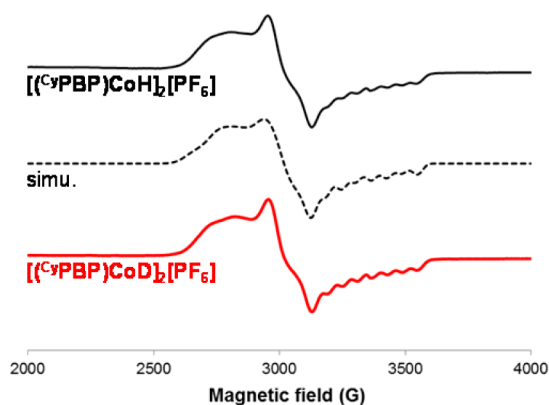
Figure 2. EPR spectra of $[(^{Cy}PBP)CoH]_2[PF_6]$ ($[2][PF_6]$, black) and $[(^{Cy}PBP)CoD]_2[PF_6]$ ($[2][PF_6]$-d_2, red) in 2-Me-THF at 77 K (9.39 GHz). Dashed trace: simulation.
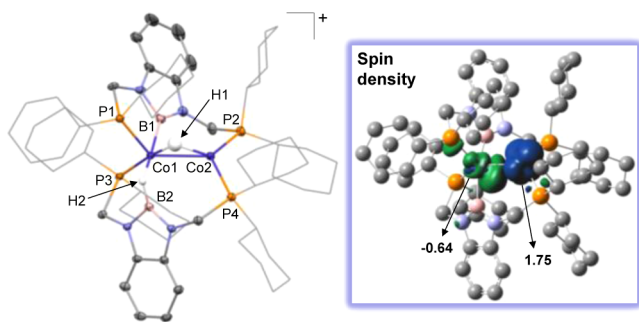

Figure 3. (left) Solid-state structure of one of the two independent molecules of $[(^{Cy}PBP)CoH]_2^+$ ($[2]^+$). Thermal ellipsoids are drawn at the 50% probability level. Cyclohexyl groups are drawn in wireframe. The counteranion, solvent molecules, and hydrogen atoms (except for the bridging hydrides) have been omitted for clarity. Pertinent metrical parameters can be found in Table 1. (right) Mulliken atomic spin density surface of $[2]^+$ (isovalue = 0.003). Hydrogen atoms have been omitted for clarity.

changes upon oxidation are the elongation of the Co2−B1 contact (3.002(4) Å in $[2]^+$ vs 2.375(2) Å in 1) and the Co2−B2 contact (3.276(3) Å in $[2]^+$ vs 2.563(2) Å in 1) (Table 1),

Table 1. Selected Bond Lengths (Å) for $[(^{Cy}PBP)CoH]_2$ (1) and $[(^{Cy}PBP)CoH]_2^+$ ($[2]^+$)

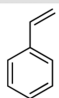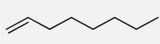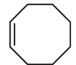|	$[(^{Cy}PBP)CoH]_2$	$[(^{Cy}PBP)CoH]_2^+$
Co1−Co2	2.3542(3)	2.4643(5)[a]
Co1−B1	2.049(2)	1.994(4)[a]
Co1−B2	2.006(2)	2.290(3)[a]
Co2−B1	2.375(2)	3.002(4)[a]
Co2−B2	2.563(2)	3.276(3)[a]
B2−H2	1.37(3)	1.19(4)[a]

[a]Average of two independent molecules.

exceeding the sum of covalent radii of the two elements (2.1 Å)[21] by 30−36%. A longer Co1−Co2 bond is measured (2.4643(5) Å in $[2]^+$ vs 2.3542(3) Å in 1). Other noteworthy variations are the longer Co1−B2 contact (2.290(3) Å in $[2]^+$ vs 2.006(2) Å in 1) and the shorter B2−H2 bond (1.19(4) Å in $[2]^+$ vs 1.37(3) Å in 1), hinting at a weakly ligated η^2-hydridoborane. This statement is reinforced by the observation of a higher-energy B−H stretching frequency in $[2]^+$ (1775 cm^{-1}) than in 1 (1651 cm^{-1}).

Figure 3 shows the Mulliken atomic spin density surface for $[2]^+$ (spin density = −0.64 on Co1 and 1.75 on Co2), which suggests that the two Co atoms are antiferromagnetically coupled. To further investigate the electronic structure, an NO analysis was performed on a simplified complex, $[(^{Me}PBP)\text{-}CoH]_2^+$ ($[2']^+$). This analysis identified magnetic interactions between two symmetry-related Co−Co bonding and antibonding orbitals (see the SI), also in agreement with two antiferromagnetically coupled Co centers.[22] The unpaired electron is located in an NO that is polarized toward Co2. This observation is consistent with the experimentally obtained EPR spectrum showing hyperfine coupling to only one Co atom.

Reversible H₂ Activation by $[(^{Cy}PBP)CoH]_2$ (1). Exposure of 1 to 1 atm H_2 in C_6D_6 immediately resulted in a color change from brown to yellow. As monitored by ^1H NMR spectroscopy, clean conversion of 1 into a new bimetallic species (hereafter denoted as 1-H_2) was confirmed. The solution magnetic moment of 1-H_2 (μ_{eff} = 2.56μ_B, 298 K, C_6D_6) is consistent with an S = 1 spin state. An alternative interpretation of the solution magnetic measurement is that 1-H_2 fully dissociates into two S = $^1/_2$ species (μ_{eff} = 1.81μ_B). However, such a monomeric S = $^1/_2$ species is supported by neither the ^1H DOSY NMR experiments (see the SI) nor the absence of an EPR signal (2-Me-THF, 77 K). The conversion between 1 and 1-H_2 is fully reversible. Subjecting a C_6D_6 solution of 1-H_2 to a few freeze−pump−thaw cycles quantitatively regenerated 1. The peak of HD was immediately observed by ^1H NMR spectroscopy when 1 was exposed to a 1:1 mixture of H_2 and D_2 (1 atm), implying rapid and reversible H_2/D_2 activation. The ATR-IR spectrum of 1-H_2 under an atmosphere of H_2 exhibited a broad B−H stretching band at 1738 cm^{-1}. The same band disappeared under D_2. Multiple attempts to crystallize 1-H_2 under an atmosphere of H_2 were not fruitful. We hypothesize that a plausible identity of 1-H_2 is a bis(hydridoborane) Co−(μ_2-H)$_2$−Co complex, $[(^{Cy}PBHP)\text{-}CoH]_2$, resulting from addition of H_2 across the boryl−Co bond. Another likely scenario is bimetallic addition, leading to bridging or terminal Co−H species. [16b] The presence of an intact H_2 ligand in 1-H_2 appears to us a less likely scenario. This assumption is based on (1) the lack of N_2 binding by 1 (toluene, −100 °C) and (2) a structurally related bimetallic boryl−Ni analogue (vide infra).

Catalytic Olefin Hydrogenation by $[(^{Cy}PBP)CoH]_2$ (1). The ability of 1 to serve as an olefin hydrogenation catalyst was initially studied as follows. Exposure of a C_6D_6 solution of 1 to 1 atm ethylene and 4 atm H_2 resulted in the immediate formation of ethane, as detected by ^1H NMR spectroscopy. Full consumption of ethylene was observed after stirring at RT for 2 h. Next, we examined bulkier olefins and compared the hydrogenation rate for 1 with that for the previously reported monomeric complex $(^{tBu}PBP)Co(N_2)$[4d] under the standard conditions (RT, 1 atm H_2, C_6D_6, 2 mol % catalyst; Table 2). Catalytic hydrogenation of styrene and 1-octene could be achieved by 1 (Table 2). However, the rates were about 2 orders of magnitude lower than those measured for $(^{tBu}PBP)\text{-}Co(N_2)$. Surprisingly, while $(^{tBu}PBP)Co(N_2)$ could not catalyze the hydrogenation of internal olefins such as cis-cyclooctene and norbornene, both alkenes were hydrogenated using 1. The solution remained transparent during the catalysis, and the reactions proceeded similarly in the presence of elemental mercury. Hydrogenation of norbornene using D_2 showed syn addition at the exo positions.[23]

13674

dx.doi.org/10.1021/ja504667f | J. Am. Chem. Soc. 2014, 136, 13672−13683

Table 2. Turnover Frequency (TOF) of Catalytic Olefin Hydrogenation by $[(^{Cy}PBP)CoH]_2$ (1) and $(^{tBu}PBP)Co(N_2)^a$

Olefin	$[(^{Cy}PBP)CoH]_2$	$(^{tBu}PBP)Co(N_2)$
(styrene)	2.5 h^{-1} (100%)	1000 h^{-1} (100%)
(1-alkene)	8 h^{-1} (92%)	1000 h^{-1} (97%)
(cyclooctene)	4 h^{-1} (100%)	0 h^{-1} (0%)
(norbornene)	5 h^{-1} (100%)	0 h^{-1} (0%)

^{a}Conditions: RT, 1 atm H_2, C_6D_6. Catalyst loading: 2 mol % relative to the olefin. The yield (given in parentheses) was determined by ^1H NMR spectroscopy using 1,3,5-trimethoxybenzene as an internal standard. The turnover frequency (h^{-1}) was calculated at the end of the reaction when the starting olefin was not detectable.

Kinetics Studies and Proposed Mechanisms. To gain insight into the mechanism, kinetic studies were performed on the hydrogenation of *cis*-cyclooctene by $[(^{Cy}PBP)CoH]_2$ (1). To this end, a series of *cis*-cyclooctene solutions (43.7 mM) containing different amounts of catalyst 1 (0.84−8.43 mM) were charged with a large excess of H_2 (3.9 atm) in J. Young NMR tubes. The progress of these reactions was then monitored by ^1H NMR spectroscopy. As shown in Figure 4,
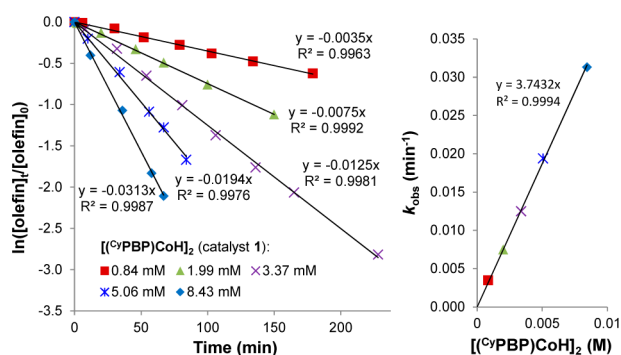

Figure 4. (left) First-order plots for the depletion of *cis*-cyclooctene (43.7 mM) in its reaction with excess H_2 (3.9 atm) catalyzed by $[(^{Cy}PBP)CoH]_2$ (1) (0.84−8.43 mM) in C_6D_6 at 298 K. (right) Plot of k_{obs} against the concentration of 1.

the olefin consumption reaction is first-order in olefin. A plot of k_{obs} against the concentration of the catalyst indicates that the reaction is first-order in 1 (the same results were obtained by the method of initial rates; see the SI).

To determine the reaction order with respect to H_2, a series of solutions of *cis*-cyclooctene (43.7 mM) and 1 (2.0 mM) in J. Young tubes were charged with different H_2 pressures (0.5−8.0 atm). These experiments indicate that the reaction is also first-order with respect to H_2 (Figure 5; see the SI for the data obtained from the method of initial rates). On the basis of the above results, with the Henry's constant for the concentration of H_2 in benzene,[24] the overall experimental rate law is

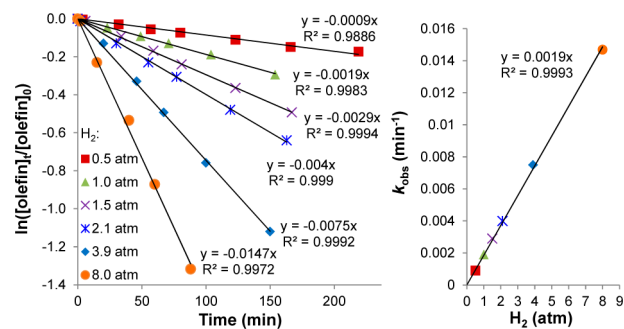$$\nu = k[\text{Co}_2][\text{S}][\text{H}_2] \quad (1)$$

Figure 5. (left) First-order plots for the depletion of *cis*-cyclooctene (43.7 mM) in its reaction with excess H_2 (0.5−8.0 atm) catalyzed by $[(^{Cy}PBP)CoH]_2$ (1) (2.0 mM) in C_6D_6 at 298 K. (right) Plot of k_{obs} against the pressure of H_2.

where $k = 123 \pm 6$ M^{-2} s^{-1}, Co_2 denotes catalyst 1, and S represents the olefin.

Three plausible mechanistic scenarios were considered in light of the aforementioned rate law (Scheme 2). During the

Scheme 2. Mechanistic Scenarios Considered for Catalytic Olefin Hydrogenation by $[(^{Cy}PBP)CoH]_2$ (1) (Co_2 = catalyst 1, S = Olefin, P = Hydrogenated Product)^a
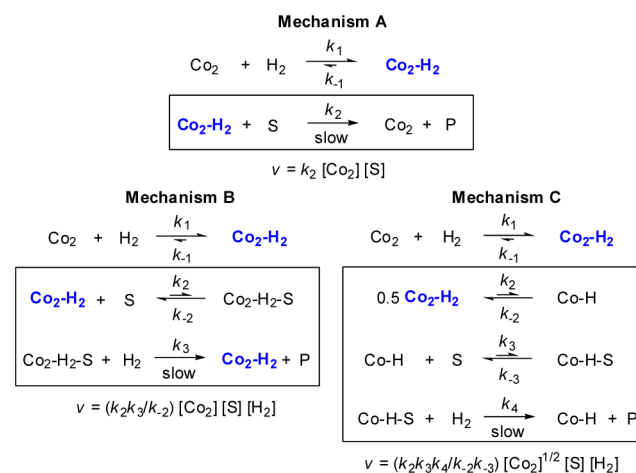
^{a}The catalyst resting state is highlighted in blue. See the SI for the derivations of the expected rate equations.

catalysis, the only observed form of the catalyst is 1-H_2 (Co_2-H_2), detected in situ by ^1H NMR spectroscopy, thus indicating a rapid equilibrium between Co_2 and Co_2-H_2 with a large equilibrium constant ($k_1/k_{-1} \gg 1$). As such, the rate law derived for mechanism A would show a zeroth-order dependence on H_2 (see the SI), which is inconsistent with the experimental observation. In turn, we propose that Co_2-H_2 is in equilibrium with the olefin adduct (Co_2-H_2-S), which then reacts with another equivalent of H_2 to yield the hydrogenated product (P) and regenerate Co_2-H_2, as shown in mechanism B. Mechanism B would lead to an overall rate expression that is first-order in Co_2, S, and H_2.[25] However, in mechanism B we cannot rule out the possibility that a pre-equilibrium between Co_2-H_2 and Co_2-H_4 occurs prior to olefin binding. Although the measured kinetic isotope effect (k_H/k_D) of 1.4 appears to indicate H−H bond cleavage in the rate-determining step,[26] we note that the observed k_H/k_D value is a combination of the isotope effects for all of the individual steps. Lastly, if Co_2-H_2 predissociates into catalytically active *monometallic* Co−H

species (mechanism C), the overall rate law should be half-order with respect to Co_2,[27] again inconsistent with the kinetic data. Taking these results collectively, we therefore propose that the overall mechanistic outline B is a highly plausible scenario. We hypothesize that the ligation of an olefin to Co_2-H_2 may require predissociation of a phosphine or a σ-borane ligand, given that Co_2-H_2 is likely an electronically saturated species (see the SI for plausible identities). That hydrogenation should proceed by a *bimetallic* instead of a monometallic boryl−Co catalyst is interesting and perhaps suggestive of metal−metal cooperativity.[28]

Synthesis of Bimetallic Boryl−Ni Complexes. Reaction of the ligand ^{Ph}**PB(H)P**[14] with $Ni(COD)_2$ (COD = cyclooctadiene) in THF afforded the bimetallic $Ni^I Ni^I$ complex $[(^{Ph}$**PBP**)**Ni**$]_2$ (**3**) in moderate yield (Scheme 3). Complex **3** is

Scheme 3. Synthesis of Complexes 3 and 4
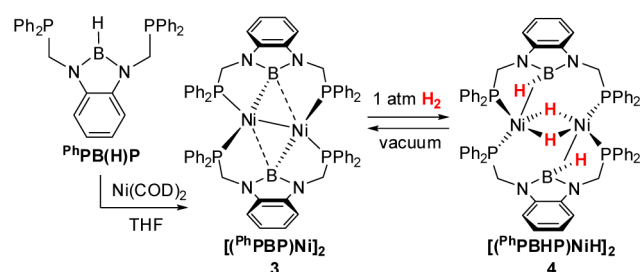
diamagnetic and is characterized by a broad ^{11}B NMR signal resonating at 42.7 ppm in THF-d_8, consistent with those observed for boryl−metal species.[11c] The ^{31}P NMR spectrum of **3** displays a singlet at 46.4 ppm. The absence of a hydride ligand in **3** is supported by the ^{1}H NMR and ATR-IR spectra.

Complex **3** crystallizes in the $P1$ space group with two independent molecules in the asymmetric unit (Figure 6).[20]
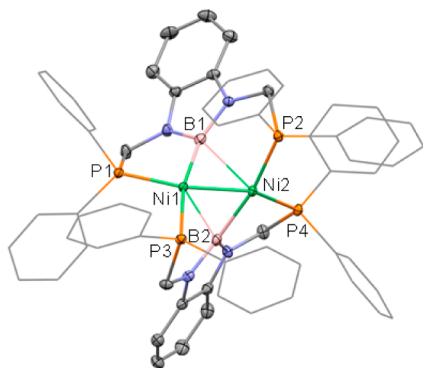
Figure 6. Solid-state structure of one of the two independent molecules of $[(^{Ph}$**PBP**)**Ni**$]_2$ (**3**). Thermal ellipsoids are drawn at the 50% probability level. Cyclohexyl groups are drawn in wireframe. Hydrogen atoms have been omitted for clarity. Selected bond lengths (averaged, Å): Ni1−Ni2 2.2421(9), Ni1−B1 2.043(6), Ni1−B2 2.368(6), Ni2−B1 2.328(6), Ni2−B2 2.046(6).

Inspection of the crystallographic structure reveals the unsymmetrical μ_2 coordination mode of two boryl ligands (Ni1−B1, 2.043(6) Å; Ni1−B2, 2.368(6) Å; Ni2−B1, 2.328(6) Å; Ni2−B2, 2.046(6) Å), leading to two square-pyramidal Ni centers. The average Ni1−Ni2 bond distance in **3** (2.2421(9) Å) is shorter than those observed for related tetrakis-(phosphino) $Ni^I Ni^I$ dimers bridged by two phosphido

(2.559(2) Å),[29] silyl (2.306−2.642 Å),[30] phenyl (2.308−2.371 Å),[31] or hydride (2.374−2.433 Å)[31] ligands. Boryl−Ni complexes are very rare, having been previously characterized only once in the solid state.[32]

Reversible H_2 Activation by $[(^{Ph}$PBP)Ni$]_2$ (3). Reaction of **3** with 1 atm H_2 in THF-d_8 at 298 K led to the rapid and quantitative formation of complex $[(^{Ph}$**PBHP**)**NiH**$]_2$ (**4**) (Scheme 3). Complex **4** features a broad ^{11}B resonance at 31.4 ppm as well as two coupled ^{31}P resonances at 47.2 and 49.1 ppm ($^2J_{P-P}$ = 60 Hz). As is evident in the ^{1}H NMR spectrum (Figure 7), complex **4** is unsymmetrical and features
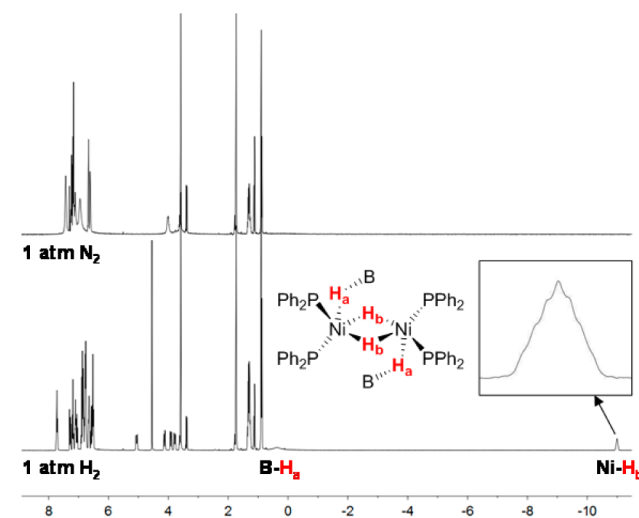
Figure 7. (top) ^{1}H NMR spectrum of $[(^{Ph}$**PBP**)**Ni**$]_2$ (**3**) in THF-d_8 under 1 atm N_2 at 298 K. (bottom) ^{1}H NMR spectrum of $[(^{Ph}$**PBHP**)**NiH**$]_2$ (**4**) in THF-d_8 under 1 atm H_2 at 298 K.

four magnetically inequivalent methylene proton resonances detected as doublets of doublets ($^2J_{H-H}$ = 13 Hz, $^2J_{P-H}$ = 7 Hz). Additionally, a broad peak (2H, 0.38 ppm) and a pseudoseptet (2H, −11.02 ppm, $^2J_{P-H}$ = 6.6 Hz, 13.2 Hz) were observed in the hydridic region. The two resonances are assigned as B−H and Ni−H, respectively, on the basis of ^{1}H{^{11}B} and ^{1}H{^{31}P} NMR experiments (see the SI). Complex **4** is diamagnetic, thus implying a dimeric species in solution. On the basis of these observations, complex **4** is best formulated as a Ni^I−(μ_2-H)$_2$−Ni^I dimer bridged by two η^2-hydridoborane ligands as a result of the addition of 2 equiv of H_2 across both boryl−Ni bonds in **3**. Accordingly, the measured T_1(min) values for both the B−H resonance (124 ms, 283 K, 500 MHz) and the Ni−H resonance (338 ms, 283 K, 500 MHz) are longer than that expected for a nonclassical H_2 adduct (see the SI).[33] When **3** was exposed to 1 atm HD, no H−D coupling was observed for either the B−H or Ni−H resonances, also arguing against the presence of a nonclassical H_2 adduct.[34] Under 1 atm H_2, a peak corresponding to free H_2 was observed in the ^{1}H NMR spectrum at room temperature. When 1:1 H_2/D_2 (1 atm) was employed, a triplet corresponding to free HD was detected immediately. The B−H and Ni−H stretching bands were not observed in the ATR-IR spectrum of **4** under H_2.

Subjecting a solution of **4** to a few freeze−pump−thaw cycles cleanly regenerated **3** as the only detectable product, a process which was monitored by multinuclear NMR spectroscopies. Reversible oxidative addition of H_2 to a Ni^I species is unprecedented. Limberg reported the irreversible reaction of a Ni^I complex with H_2, affording a Ni^{II}−(μ_2-H)$_2$−Ni^{II} dimer.[35]

Stryker also showed the irreversible reaction of $[(^{tBu}PN)Ni^I]_4$ (Chart 1) with H_2, generating unknown hydride species.[4f] As such, the present system emphasizes the significance of boryl–metal cooperativity in facile and reversible H_2 activation. We speculate that the cooperative boryl–Ni framework helps to circumvent irreversible one-electron reactions, as observed for other Ni^I species.[31a,35] The re-formation of a covalent boryl–Ni bond provides a thermodynamic driving force for the reverse reaction. For the conversion of **3** to **4**, plausible reaction pathways include (1) concerted σ-bond metathesis and (2) oxidative addition at Ni followed by reductive elimination at the Ni–B bond. In terms of broader context, it is also interesting to note that a mechanism involving oxidative addition of H_2 by a Ni^I intermediate has recently been proposed for the [NiFe]-hydrogenase active site.[36]

DFT Investigations. To gain more insight into the bonding in $[(^{Ph}PBP)Ni]_2$ (**3**) and $[(^{Ph}PBHP)NiH]_2$ (**4**), simplified model complexes $[(^{Me}PBP)Ni]_2$ (**3′**) and $[(^{Me}PBHP)NiH]_2$ (**4′**) featuring dimethyl substituents on the phosphorus atoms were examined by density functional theory (DFT). The optimized geometry of **3′** (Ni–Ni 2.273 Å) closely resembles the crystallographic structure of **3** (Ni–Ni 2.242 Å). In complex **3′**, a Ni–Ni σ bond and a four-center four-electron Ni–$(\mu_2$-B$)_2$–Ni bonding interaction are supported by the molecular orbitals (MOs) as well as an atoms in molecules (AIM)[37] analysis (see the SI). The geometry optimization of **4′** yielded a C_2-symmetric structure (Figure 8). Inspection of the LUMO reveals a σ^*(Ni–H) orbital, thus suggesting the presence of a four-center bonding interaction in the Ni–$(\mu_2$-H$)_2$–Ni unit. The bonding situation in **4′** can be further elucidated with the qualitative MO diagrams obtained from linear combinations of symmetry-relevant atomic orbitals (Figure 8). All of the depicted MOs are supported by the DFT calculations, including the HOMO, which is a π^*(Ni–Ni) orbital. Since the two electrons provided by the two Ni^I centers are paired in the π^*(Ni–Ni) orbital, no net Ni–Ni bond is present.[17b] We also note that the Ni–Ni separation in **4′** (2.631 Å) exceeds those measured for other related Ni^I–$(\mu_2$-H$)_2$–Ni^I species (2.374–2.441 Å)[31,38] in which a similar bonding situation could be envisioned (see the SI). Lastly, the agostic σ-borane coordination mode is in agreement with our calculations (see the SI).

Synthesis of Monometallic Boryl–Ni Complexes. The bimetallic complex $[(^{Ph}PBP)Ni]_2$ (**3**) is not a precatalyst for the hydrogenation of ethylene. As monitored by ^1H NMR spectroscopy, the complex's resting state in the presence of ethylene (1 atm) and H_2 (4 atm) is $[(^{Ph}PBHP)NiH]_2$ (**4**), which is a diamagnetic, electronically saturated 19-electron/19-electron species. For this reason, we pursued a monomeric boryl–Ni system by reacting the ligand $^{tBu}PB(H)P$[39] with $NiCl_2(DME)$ (DME = dimethoxyethane) in THF (Scheme 4). This reaction proceeded cleanly to give the monomeric complex $(^{tBu}PBP)NiCl$ (**5**) in moderate yield. Chloride abstraction from **5** with AgOTf (OTf = trifluoromethanesulfonate) in THF gave $(^{tBu}PBP)NiOTf$ (**6**) in quantitative yield. Synthesis of the boryl–Ni hydride species $(^{tBu}PBP)NiH$ (**7**) was accomplished by treatment of **6** with $^iPr_2Mg$ in toluene. The ^{11}B NMR resonance of **7** (47.6 ppm) appears at lower field compared with those for **5** (38.2 ppm) and **6** (31.6 ppm). The same trend is also observed in the ^{31}P NMR spectra of these complexes (**5**, 85.9 ppm; **6**, 83.6 ppm; **7**, 122.5 ppm). The ^1H NMR spectrum of **7** features a triplet at −1.69 ppm ($^2J_{P–H}$ = 34.6 Hz) that is assigned to the terminal Ni–H resonance.
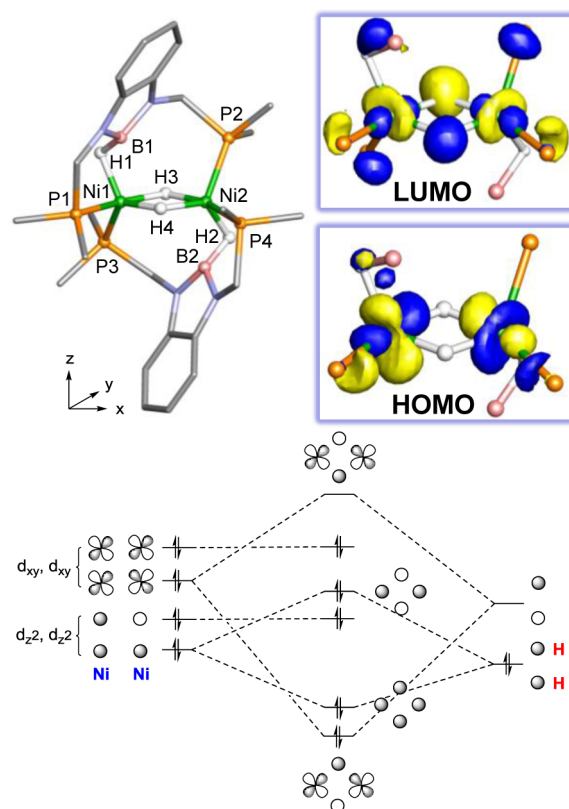
Figure 8. (top left) DFT-optimized structure of $[(^{Me}PBHP)NiH]_2$ (**4′**). Hydrogen atoms (except for the bridging hydrides) have been omitted for clarity. Selected bond lengths (Å): Ni1–Ni2 2.631, Ni1–B1 2.088, Ni1–H1 1.659, Ni1–H3 1.619, Ni1–H4 1.630, Ni2–B2 2.101, Ni2–H2 1.668, Ni2–H3 1.620, Ni2–H4 1.627. (top right) Plots of the LUMO and HOMO (isovalue = 0.05). (bottom) Qualitative MO diagrams illustrating the orbitals involved in the Ni–$(\mu_2$-H$)_2$–Ni core.

Scheme 4. Synthesis of Complexes 5, 6, 7, and 8
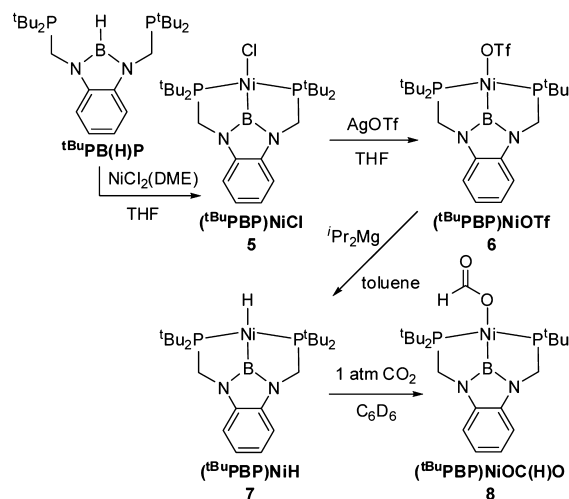
Accordingly, the Ni–H stretching band is observed at 1648 cm^{-1} and shifts to 1196 cm^{-1} (calcd 1176 cm^{-1}) upon isotopic labeling with deuterium.

The facile insertion of CO_2 into a Ni^{II}–H bond is well-known.[40] While less hydridic Ni^{II}–H species featuring an amido group trans to the hydride fail to react with CO_2, the insertion proceeds rapidly for phenyl and silyl Ni^{II}–H analogues.[40c–g]

13677

dx.doi.org/10.1021/ja504667f | J. Am. Chem. Soc. 2014, 136, 13672–13683

Since boryl ligands are known to engender a very strong trans influence,[12] it was not surprising that **7** rapidly reacted with CO_2 (1 atm) to give the formate complex (tBuPBP)NiOC-(H)O (**8**). Complex **8** was characterized by ^{11}B and ^{31}P resonances at 35.7 and 85.2 ppm, respectively. The C−H resonance of the Ni-bound formate was detected at 9.11 ppm as a singlet. The ATR-IR spectrum of **8** exhibited two bands at 1619 and 1323 cm^{-1} that are assigned to the antisymmetric and symmetric C−O stretches, respectively. The energetic difference of 296 cm^{-1} between these two stretches is consistent with a κ^1-O-formate,[41] as confirmed by the solid-state structure.

The solid-state structures of complexes **5**−**8** were determined by X-ray crystallography (Figure 9). In all cases, the Ni
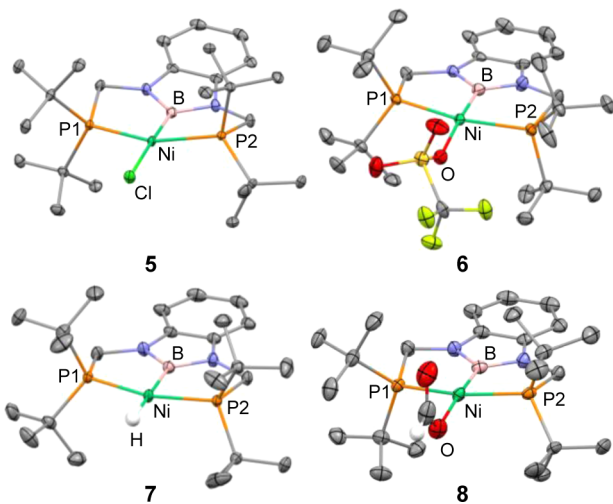
Figure 9. Solid-state structures of (tBuPBP)NiCl (**5**), (tBuPBP)NiOTf (**6**), (tBuPBP)NiH (**7**), and (tBuPBP)NiOC(H)O (**8**). Thermal ellipsoids are drawn at the 50% probability level. Solvent molecules and hydrogen atoms (except for the Ni−H in **7** and the formate C−H in **8**) have been omitted for clarity. Pertinent metrical parameters can be found in Table 3.

centers adopt pseudo-square-planar geometries, as indicated by the P1−Ni−P2 and B−Ni−X angles (X = Cl (**5**), O (**6**), H (**7**), O (**8**); Table 3). The measured Ni−B distances in these complexes are very similar (1.905−1.907 Å), seemingly because of the rigid tridentate ligand scaffold. The strong trans influence of the boryl group can be inferred by comparing the Ni−Cl bond distance in **5** (2.2399(4) Å) with those measured for bis(phosphino) Ni^{II}−Cl complexes featuring trans amino (2.169 Å),[5c] pyridinyl (2.160−2.164 Å),[42] phenyl (2.181−2.242 Å),[43] alkyl (2.213−2.249 Å),[43c,44] and silyl (2.242−2.265 Å)[40e,45] groups. The hydride ligand in **7** is located 1.53(4) Å away from Ni. This Ni−H bond distance falls within those measured for related Ni^{II}−H complexes (1.37−1.60 Å).[43e,46]

Catalytic Olefin Hydrogenation by (tBuPBP)NiH (7).

The capability of **7** to catalyze olefin hydrogenation was examined as follows. A J. Young NMR tube containing a C_6D_6 solution of an olefin and catalyst **7** was charged with 1 atm H_2. The progress of the reaction was then monitored by ^1H NMR spectroscopy. The TOFs and yields are summarized in Table 4.

Table 4. Turnover Frequency (TOF) of Catalytic Olefin Hydrogenation by (tBuPBP)NiH (7), (tBuPCP)NiH, and (CyPNHP)NiH$^+$

	(tBuPBP)NiH	(tBuPCP)NiH	(CyPNHP)NiH$^+$
Conditions:	1 atm H_2, RT	1 atm H_2, RT	4 atm H_2, 80 °C
styrene	25 h^{-1} (100%)^a	0.7 h^{-1} (100%)^a	0.4 h^{-1} (100%)^b
1-octene	25 h^{-1} (64%)^a	0 h^{-1} -^{a}	0.4 h^{-1} (70%)^b
3,3-dimethyl-1-butene	5 h^{-1} (100%)^a	0 h^{-1} -^{a}	0.2 h^{-1} (97%)^b
cyclooctene	0.6 h^{-1} (100%)^a	0 h^{-1} -^{a}	not reported

^{a}Conditions: 2 mol % catalyst relative to olefin, C_6D_6. The yield (given in parentheses) was determined by ^1H NMR spectroscopy using 1,3,5-trimethoxybenzene as an internal standard. The turnover frequency (h^{-1}) was calculated at the end of the reaction when the starting olefin was not detectable. ^{b}As reported by Hanson:[5c] 10 mol % catalyst relative to olefin, THF-d_8.

Under the standard conditions (RT, 1 atm H_2, C_6D_6, 2 mol % catalyst), styrene was fully hydrogenated to ethylbenzene with a TOF of 25 h^{-1}. A 64% yield was obtained for the hydrogenation of 1-octene to *n*-octane in 1.3 h. The lower yield is due to olefin isomerization, yielding internal alkenes that were not hydrogenated at RT. The hydrogenation of internal octenes could be achieved in 2 h by warming the reaction mixture to 60 °C. 3,3-Dimethyl-1-butene (TOF = 5 h^{-1}) and *cis*-cyclooctene (TOF = 0.6 h^{-1}) were fully hydrogenated at lower rates under the standard conditions. During the catalysis, the color of the solution remained yellow and transparent. All of the hydrogenation reactions proceeded similarly in the presence of elemental Hg.

Table 3. Selected Bond Lengths (Å) and Angles (deg) for (tBuPBP)NiCl (5), (tBuPBP)NiOTf (6), (tBuPBP)NiH (7), and (tBuPBP)NiOC(H)O (8)

	5	6	7	8
Ni−B	1.907(2)	1.907(4)^a	1.907(2)^a	1.905(3)
Ni−X^b	2.2399(4)	2.034(3)^a	1.53(4)^a	1.958(2)
Ni−P	2.2091(6)^a	2.236(1)^a	2.153(1)^a	2.217(1)^a
P1−Ni−P2	156.995(18)	158.23(4)^a	160.24(2)^a	158.92(3)
B−Ni−X^b	178.20(6)	173.21(16)^a	178.55(11)^a	173.54(12)

^{a}An averaged value. ^{b}X = Cl (**5**), O (**6**), H (**7**), O (**8**).

While Ni is frequently employed as a heterogeneous hydrogenation catalyst,[47] homogeneous Ni-based olefin hydrogenation catalysts remain rare,[4f,5] with some requiring high H_2 pressure (50 bar) to achieve turnover.[5a,b] To further evaluate the effects of the boryl functionality in catalytic hydrogenation reactions, the phenyl analogue of 7, (^{tBu}PCP)NiH,[46b] was independently prepared and subjected to the standard hydrogenation conditions. As shown in Table 4, (^{tBu}PCP)NiH operates at a lower rate for styrene and is inactive for the other olefins under the same conditions. Hanson recently synthesized a related amino analogue, (^{Cy}PNHP)NiH$^+$.[5c] Compared with those for 7, the reported rates for (^{Cy}PNHP)NiH$^+$ are lower even at 80 °C under 4 atm H_2.

Kinetics Studies and Proposed Mechanisms. A plausible scenario for the hydrogenation reactions catalyzed by (^{tBu}PBP)NiH (7) is mechanism A in Scheme 5. Migratory

Scheme 5. Mechanistic Scenarios Considered for Catalytic Olefin Hydrogenation by (^{tBu}PBP)NiH (7) (Ni-H = catalyst 7, S = Olefin, P = Hydrogenated Product)[a]

Mechanism A	Mechanism B
Ni-H + S $\underset{k_{-1}}{\overset{k_1}{\rightleftharpoons}}$ Ni-H-S	Ni-H + S $\underset{k_{-1}}{\overset{k_1}{\rightleftharpoons}}$ Ni· + HS·
Ni-H-S + H$_2$ $\overset{k_2}{\longrightarrow}$ Ni-H + P	Ni-H + HS· $\overset{k_2}{\longrightarrow}$ Ni· + P
	2 Ni· + H$_2$ $\underset{k_{-3}}{\overset{k_3}{\rightleftharpoons}}$ 2 Ni-H
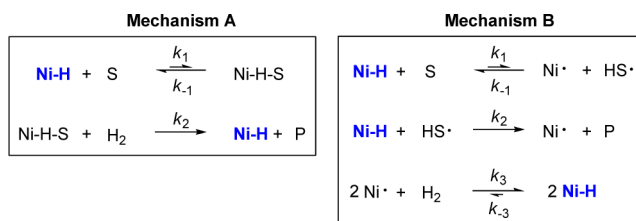
[a]The catalyst resting state is highlighted in blue.

insertion of the olefin (S) into the Ni−H bond would give a Ni−alkyl intermediate (Ni-H-S). This reaction is expected to be reversible since the reaction of (^{tBu}PBP)NiOTf (6) with $^iPr_2Mg$ yields 7, presumably via β-hydride elimination from a transiently formed Ni-^iPr species. Ni-H-S would then react with H_2 to give the hydrogenated product (P) and regenerate catalyst 7 (Ni-H). Since 7 is the only observable resting state of the catalyst under this scheme, the derived rate law using the steady-state approximation for Ni-H-S is

$$v = \frac{k_1 k_2 [\text{Ni-H}][\text{S}][\text{H}_2]}{k_{-1} + k_2 [\text{H}_2]} \tag{2}$$

In line with this rate expression, our kinetic studies indicate a first-order dependence on both 7 (Ni-H) and *cis*-cyclooctene (Figure 10a,b). The reaction is expected to be first-order with respect to H_2 for $k_{-1} \gg k_2[\text{H}_2]$ and zeroth-order for $k_{-1} \ll k_2[\text{H}_2]$. In turn, a fractional-order dependence on H_2 is observed (Figure 10c), thus indicating that neither k_{-1} nor $k_2[\text{H}_2]$ is negligible within the range of H_2 pressures employed in these experiments (0.3−3.9 atm). The double-reciprocal form of eq 2 can be rearranged as

$$\frac{1}{v} = \frac{k_{-1}}{k_1 k_2 [\text{Ni-H}][\text{S}][\text{H}_2]} + \frac{1}{k_1 [\text{Ni-H}][\text{S}]} \tag{3}$$

A plot of $1/v$ against $1/[\text{H}_2]$ (Figure 10d) yields a straight line. The value of k_1 (0.16 M^{-1} s^{-1}) and the k_{-1}/k_2 ratio (0.005 M) can therefore be estimated according to eq 3. The intermediacy of a Ni−alkyl species (Ni-H-S) is consistent with an overall k_H/k_D value of 0.8. The inverse kinetic isotope effect could be attributed to the difference in zero-point energy, which is more
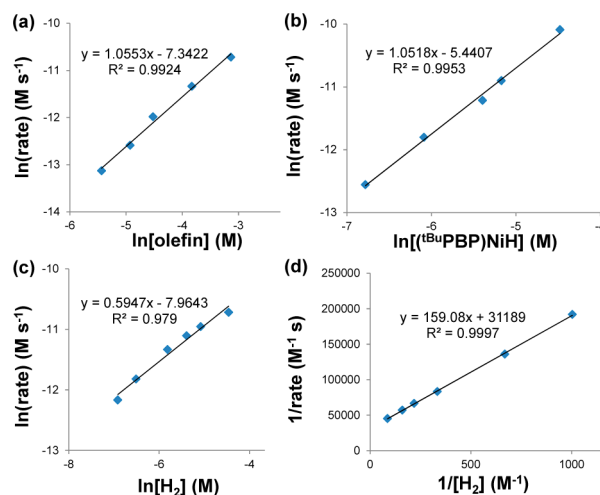

Figure 10. Reaction order determination by the method of initial rates for the hydrogenation of *cis*-cyclooctene catalyzed by (^{tBu}PBP)NiH (7). (a) Plot of ln(rate) against ln[olefin] ([olefin] = 4.36−43.6 mM). (b) Plot of ln(rate) against ln[Ni-H] ([Ni-H] = 1.14−11.4 mM). (c) Plot of ln(rate) against ln[H$_2$] (pressure of H$_2$ = 0.3−3.9 atm). (d) Plot of 1/rate against 1/[H$_2$].

pronounced for the C−H(D) bond than for the Ni−H(D) bond,[48] leading to a larger k_1 when D_2 is employed.

The other mechanism shown in Scheme 5 involves stepwise hydrogen atom transfer from Ni-H to the olefin (mechanism B).[49] Turnover can be achieved by reaction of the two generated Ni· species with H_2. However, under an atmosphere of N_2, no reaction was observed between 7 (Ni-H) and excess *cis*-cyclooctene over several days in C_6D_6, thus ruling out the possibility of a hydrogen atom transfer pathway. Lastly, the reaction of norbornene with D_2 catalyzed by 7 gave exclusively the syn addition product,[23] which cannot rule out mechanism B but is more consistent with mechanism A.

The mechanistic studies offer a reasonable explanation for the observation that (^{tBu}PBP)NiH (7) is a more active olefin hydrogenation catalyst than its phenyl and amino analogues, with the assumption that all these species follow a similar mechanistic pathway.[50] The strong trans influence of the boryl group[12] would be expected to destabilize the Ni−H and Ni−alkyl bonds, thus leading to kinetically more favorable migratory insertion (k_1) and σ-bond metathesis (k_2) steps. The presence of a weaker Ni−H bond in 7 is also supported by the observation of an unusually low Ni−H stretching frequency in 7 (1648 cm^{-1}) versus (^{tBu}PCP)NiH (1754 cm^{-1})[46b] and (^{Cy}PNHP)NiH$^+$ (1886 cm^{-1}).[5c]

■ CONCLUSION

We have shown that a bis(phosphino)boryl auxiliary ligand, originally introduced by Nozaki and Yamashita, facilitates rapid and reversible H_2 activation reactions in Co and Ni complexes, for example, reversible H_2 activation by the S = 1 bimetallic Co complex [(^{Cy}PBP)CoH]$_2$ (1). The ability of 1 to serve as an olefin hydrogenation catalyst has been investigated, and kinetic studies indicate that the rate-limiting step likely involves a bimetallic Co species. Whereas 1 hydrogenates terminal olefins more slowly than its monomeric relative (^{tBu}PBP)CoN$_2$, it is curiously more active toward internal olefins. The bimetallic Ni complex [(^{Ph}PBP)Ni]$_2$ (3) featuring two unsymmetrical bridging boryl ligands has also been prepared. Reaction of 3 with 1 atm H_2 affords the Ni^I−(μ$_2$-H)$_2$−Ni^I complex

$[(^{Ph}PBHP)Ni]_2$ (**4**) as a result of the addition of 2 equiv of H_2 across the boryl−Ni bonds. The facile and reversible H_2 activation by a Ni^I species was previously unknown and has been herein attributed to boryl−Ni cooperativity. By contrast to the bimetallic Co catalyst **1**, the bimetallic Ni complex **3** is inactive for olefin hydrogenation (e.g., ethylene, 4 atm H_2, RT). However, monometallic boryl−Ni complexes show enhanced catalytic activity. For example, the boryl−Ni hydride complex $(^{tBu}PBP)NiH$ (**7**) can be exploited in the context of olefin hydrogenation. Kinetic data on hydrogenation reactions of this system are consistent with reversible olefin insertion into the Ni−H bond followed by hydrogenolysis. It is interesting to note that complex **7** is a more active olefin hydrogenation catalyst compared with its isoelectronic/isostructural phenyl and amino analogues. We attribute this enhanced catalytic activity to the strong trans influence exerted by the boryl ligand.

The present study highlights the beneficial effects of boryl ligands in reversible H_2 activation chemistry and catalytic olefin hydrogenation. The use of a strong-field boryl ligand that facilitates E−H bond activation across the metal−boryl bond constitutes a promising approach for the design of base-metal catalysts in multielectron reductive reactions.

■ EXPERIMENTAL SECTION

General Considerations. Ligands $^{Ph}PB(H)P$, $^{Cy}PB(H)P$, and $^{tBu}PB(H)P$ were prepared according to the reported procedures.[14,39] $^iPr_2Mg$ was prepared according to the known procedure.[51] Solvents were dried by passing them through an activated alumina column (*n*-pentane, benzene, toluene, Et_2O, and THF). Deuterated solvents were purchased from Cambridge Isotope Laboratories and were degassed and stored over activated 3 Å molecular sieves prior to use. CoI_2, Na, Hg, $FcPF_6$, $Ni(COD)_2$, $NiCl_2(DME)$, and AgOTf were purchased from Aldrich and used as received. Elemental analyses were performed by Midwest Microlab (Indianapolis, IN).

Spectroscopic Measurements. Ambient-temperature NMR spectra were recorded on Varian 300, 400, and 500 MHz NMR spectrometers. Chemical shifts (δ) are given in parts per million and are referenced against residual solvent signals (^1H, ^{13}C) or external BF_3−Et_2O (^{11}B, ^{19}F) and H_3PO_4 (^{31}P). T_1(min) values were determined by fitting the pulse-recovery ^1H spectra at various temperatures using the T_1 calculation protocols in either Varian's VnmrJ software or Mestrelab Research S.L.'s Mestrenova version 6.2.1. EPR spectra were recorded on a Bruker EMS spectrometer at ~2 mM concentrations. The ATR-IR measurements were obtained on a thin film of the complex obtained from evaporating a drop of the solution on the surface of a Bruker ALPHA ATR-IR spectrometer probe (Platinum Sampling Module, diamond, OPUS software package) at 2 cm^{-1} resolution. Solution IR measurements were obtained in KBr pellets using a Bio-Rad Excalibur FTS 3000 spectrometer with Varian Resolutions Pro software.

Catalytic Hydrogenation of Olefins. A J. Young NMR tube was charged with the olefin and the catalyst (8 mM, 2% mol relative to the olefin) in C_6D_6. The tube was subjected to one freeze−pump−thaw cycle on a high-vacuum line. After the tube was backfilled with 1 atm H_2, it was immediately sealed, frozen with liquid nitrogen, and brought to the spectrometer. The progress of the reaction was then monitored by ^1H NMR spectroscopy. The yields were determined by integration of the olefinic ^1H resonances against an internal standard (1,3,5-trimethoxybenzene). The identities of the hydrogenated products were established by ^1H and ^{13}C NMR spectroscopies as well as GC analysis. Control experiments carried out under the same conditions in the presence Hg showed essentially identical results. Control experiments carried out in the absence of catalyst indicated no reactivity.

Kinetic Studies of Catalytic Olefin Hydrogenation. A J. Young NMR tube was charged with catalyst (**1** or **7**), *cis*-cyclooctene, and an internal standard (1,3,5-trimethoxybenzene) in C_6D_6. The tube was subjected to one freeze−pump−thaw cycle on a high-vacuum line.

After the tube was backfilled with H_2, it was immediately sealed, frozen with liquid nitrogen, and brought to the spectrometer. For a higher pressure, the entire NMR tube was cooled to 195, 143, or 77 K and then backfilled with 1 atm H_2, leading to a pressure of 1.5, 2.1, or 3.9 atm after the sealed tube warmed to 298 K. The progress of these reactions was monitored by ^1H NMR spectroscopy. In order to achieve stirring, the tube was rotated at 10−15 rpm when spectra were not being collected. To maintain a constant H_2 pressure, the amount of H_2 was a large excess with respect to *cis*-cyclooctene.

Crystallographic Measurements. The crystallographic measurements were performed at 100(2) K using a Bruker APEX-II CCD area detector diffractometer (Mo Kα radiation, λ = 0.71073 Å). In each case, a specimen of suitable size and quality was selected and mounted onto a nylon loop. The structures were solved by direct methods, which successfully located most of the non-hydrogen atoms. Semiempirical absorption corrections were applied.[52] Subsequent refinement on F^2 using the SHELXTL/PC package (version 6.1) allowed the remaining non-hydrogen atoms to be located.[53]

Computational Details. DFT structural optimizations were performed without any symmetry restraints using the Gaussian 03 suite of programs[54] with the BP86[55] functional and a 6-31+G(d,p) basis set on all atoms. No instability was found in the optimized wave function with respect to relaxation of various constraints. Frequency calculations performed on the optimized structures indicated the absence of imaginary vibrational frequencies. The optimized structures were plotted using Gaussview or Jimp 2.[56] The topologies of the electron densities for **3′** and **4′** were subjected to an AIM[37] calculation using AIM2000.[57]

Synthesis of $[(^{Cy}PBP)CoH]_2$ (1). To a THF solution (10 mL) of CoI_2 (280.3 mg, 0.896 mmol) was added a THF solution (5 mL) of $^{Cy}PB(H)P$ (482.6 mg, 0.896 mmol). The mixture was allowed to stir at RT for 30 min, affording a greenish-yellow solution. To this mixture was added a THF suspension of sodium amalgam (Na: 42.2 mg (1 wt % Hg), 1.837 mmol). The mixture was subjected to rapid stirring for 24 h at RT, yielding a brown solution. The solvent was removed under reduced pressure. The product was extracted into pentane (5 mL × 3) and filtered through a plug of Celite. Recrystallization by slow concentration of the pentane solution afforded dark crystals of **1**, which were dried under vacuum (430 mg, 80%). Crystals suitable for X-ray diffraction analysis were obtained from diffusion of pentane into a concentrated benzene solution of **1**. ^1H NMR (400 MHz, C_6D_6): δ −11.78, −4.57, −3.82, −2.45, −1.84, −0.90, −0.25, −0.05, 0.27, 1.68, 2.04, 4.91, 5.80, 9.89, 10.44, 17.49, 21.90, 77.92. Solution magnetic moment (298 K, C_6D_6): 2.81μ_B. ATR-IR: $\nu_{B−H}$ = 1651 cm^{-1}. Elemental analysis calculated (%) for **1** ($C_{64}H_{106}B_2Co_2N_4P_4$): C, 64.33; H, 8.94; N, 4.69. Found: C, 64.04; H, 9.43; N, 4.37.

Reversible Reaction of $[(^{Cy}PBP)CoH]_2$ (1) with H_2. A C_6D_6 solution of **1** in a J. Young NMR tube was subjected to one freeze−pump−thaw cycle and then backfilled with 1 atm H_2. The ^1H NMR spectrum of the resulting sample within 5 min confirmed the quantitative consumption of **1** and the formation of $[(^{Cy}PBHP)CoH]_2$ (**1**-H_2). Subjecting the resulting sample to three freeze−pump−thaw cycles led to quantitative regeneration of **1**. Characterizations obtained for **1**-H_2: ^1H NMR (400 MHz, C_6D_6): δ −8.26, −3.33, −1.85, −1.24, −0.88, −0.43, 0.00, 0.21, 0.30, 0.87, 1.12, 1.25, 1.42, 1.54, 1.60, 1.71, 2.05, 2.75, 3.27, 3.59, 4.32, 4.54, 5.00, 7.58, 8.46, 8.89, 10.96, 13.59, 21.21, 26.51, 37.28, 55.03. Solution magnetic moment (298 K, C_6D_6): 2.56μ_B. ATR-IR: $\nu_{B−H}$ = 1738 cm^{-1}. Elemental analysis on this compound was not performed because of the loss of H_2.

Synthesis of $[(^{Cy}PBP)CoH]_2[PF_6]$ ([2][PF_6]). To a THF suspension (5 mL) of $FcPF_6$ (33.2 mg, 0.100 mmol) was added a THF solution (5 mL) of complex **1** (120 mg, 0.100 mmol) at −78 °C. The mixture was allowed to slowly warm to RT over a period of 2 h and stirred at RT for 15 h, affording a brown solution. Removal of solvents gave a dark residue that was washed with Et_2O (5 mL × 3) to give a red solid. THF (10 mL) was added, and the solution was filtered through a short plug of Celite. Slow Et_2O diffusion into the resulting THF solution gave dark-red crystals of **[2][PF_6]** (65 mg, 48%). ^1H NMR (400 MHz, THF-d_8): δ −34.22, −29.10, −23.33, −21.25, −15.65, −14.73, −14.08, −9.52, −9.22, −8.10, −6.55, −4.30, −4.05,

−3.96, −3.83, −3.45, −2.73, −2.65, −2.35, −2.25, −2.22, −2.16, −1.98, −1.49, −0.90, −0.57, −0.19, 0.36, 0.54, 1.09, 1.23, 1.44, 1.59, 1.67, 1.80, 2.06, 2.20, 2.60, 3.25, 3.39, 3.56, 4.00, 5.35, 6.48, 8.67, 8.95, 12.72, 14.28, 16.56, 26.20, 59.11, 99.85. Solution magnetic moment (298 K, THF-d_8): 1.62μ_B. ATR-IR: ν_{B-H} = 1775 cm^{-1}. Satisfactory elemental analysis could not be obtained for this compound. MS (ESI$^+$): calcd for [**2**]$^+$ ($C_{64}H_{106}B_2Co_2N_4P_4^+$) 1194.6, found 1194.6.

Synthesis of [(^{Ph}PBP)Ni]$_2$ (3). To a THF solution (5 mL) of Ni(COD)$_2$ (57.1 mg, 0.208 mmol) was added a THF solution of ligand ^{Ph}PB(H)P (106.8 mg, 0.208 mmol) dropwise at RT. The resulting mixture was allowed to stir at RT for 12 h, leading to a homogeneous red solution. On this THF solution was carefully layered 10 mL of pentane. After 12 h, dark-red crystals of **3** were obtained by filtration, washed with pentane (5 mL × 3), and dried under vacuum (88 mg, 74%). When the reaction was carried out in C_6D_6, a ^{1}H resonance corresponding to free H$_2$ was observed within 10 min in the ^{1}H NMR spectrum. ^{1}H NMR (400 MHz, THF-d_8): δ 3.60 (bs, 4H), 4.01 (bs, 4H), 6.61 (bs, 4H), 6.67 (bs, 4H), 6.94 (bs, 16H), 7.09−7.30 (m, 16H), 7.42 (bs, 8H). ^{31}P{^{1}H} NMR (161.8 MHz, THF-d_8): δ 46.4. ^{11}B{^{1}H} NMR (128.4 MHz, THF-d_8): δ 42.7 (the ^{11}B resonance shows the same line width). ^{13}C{^{1}H} NMR (100.5 MHz, THF-d_8): δ 107.51, 117.41, 128.31, 128.85, 129.82, 131.20, 134.30, 137.39, 140.65. Elemental analysis calculated (%) for **3** ($C_{64}H_{56}B_2N_4Ni_2P_4$): C, 67.19; H, 4.93; N, 4.90. Found: C, 66.64; H, 5.65; N, 4.72.

Synthesis of [(^{Ph}PBHP)NiH]$_2$ (4). A J. Young NMR tube containing a THF-d_8 solution of **3** was subjected to one freeze−pump−thaw cycle and then backfilled with 1 atm H$_2$. Rapid and quantitative formation of **4** was confirmed by multinuclear NMR spectroscopies. ^{1}H NMR (400 MHz, THF-d_8): δ −11.02 (tt, NiH, 2H, $^2J_{P-H}$ = 6.6 Hz, 13.2 Hz), 0.38 (s, BH, 2H), 3.78 (dd, 2H, $^2J_{H-H}$ = 13.2 Hz, $^2J_{P-H}$ = 6.9 Hz), 3.91 (dd, 2H, $^2J_{H-H}$ = 13.2 Hz, $^2J_{P-H}$ = 6.9 Hz), 4.12 (dd, 2H, $^2J_{H-H}$ = 13.2 Hz, $^2J_{P-H}$ = 6.9 Hz), 5.06 (dd, 2H, $^2J_{H-H}$ = 13.2 Hz, $^2J_{P-H}$ = 6.9 Hz), 6.50−6.59 (m, 8H), 6.65 (t, $^2J_{P-H}$ = 7.8 Hz, 4H), 6.74−6.91 (m, 20H), 7.03−7.12 (m, 6H), 7.19 (t, $^2J_{P-H}$ = 7.7 Hz, 4H), 7.27 (t, $^2J_{P-H}$ = 7.2 Hz, 2H), 7.72 (t, $^2J_{P-H}$ = 7.5 Hz, 4H). ^{31}P{^{1}H} NMR (161.8 MHz, THF-d_8): δ 47.2 ($^2J_{P-P}$ = 60 Hz), 49.1 ($^2J_{P-P}$ = 60 Hz). ^{11}B{^{1}H} NMR (128.4 MHz, THF-d_8): δ 31.4. ^{13}C{^{1}H} NMR (100.5 MHz, THF-d_8): δ 108.22 (d, J_{P-P} = 36.1 Hz), 117.92 (d, J_{P-P} = 27.8 Hz), 127.54, 127.60, 127.85, 128.00, 128.03, 128.06, 128.35, 128.39, 128.45, 128.54, 128.68, 128.81, 129.55 (d, J_{P-P} = 21.2 Hz), 130.34, 130.39, 130.44, 132.57 (d, J_{P-P} = 12.6 Hz), 134.03 (d, J_{P-P} = 13.2 Hz), 134.65 (d, J_{P-P} = 14.0 Hz), 135.62 (d, J_{P-P} = 26.2 Hz), 138.97 (d, J_{P-P} = 23.8 Hz), 140.79 (t, J_{P-P} = 19.1 Hz), 142.16 (d, J_{P-P} = 24.1 Hz). Elemental analysis on this compound was not performed because of the loss of H$_2$.

Synthesis of (^{tBu}PBP)NiCl (5). THF (15 mL) was added to a flask containing ligand ^{tBu}PB(H)P (1.596 g, 3.675 mmol) and NiCl$_2$(DME) (0.848 g, 3.859 mmol) at RT. The reaction mixture was stirred for 2 h, leading to the formation of a green solid suspended in a yellow solution. The green solid was removed by filtration. Removal of solvent from the filtrate gave **5** as a yellow solid that was washed with cold pentane (5 mL × 3) and dried under vacuum (1.2 g, 62%). Yellow crystals of **5** were obtained by slow concentration of a pentane solution of **5**. ^{1}H NMR (400 MHz, C_6D_6): δ 1.67 (t, 36H, $^3J_{P-H}$ = 6.7 Hz), 3.54 (t, 4H, $^2J_{P-H}$ = 2.0 Hz), 6.91 (dd, 2H, J_{H-H} = 5.6 Hz, J_{H-H} = 3.3 Hz), 7.13 (dd, 2H, J_{H-H} = 5.6 Hz, J_{H-H} = 3.3 Hz). ^{31}P{^{1}H} NMR (161.8 MHz, C_6D_6): δ 85.9. ^{11}B{^{1}H} NMR (128.4 MHz, C_6D_6): δ 38.2. ^{13}C{^{1}H} NMR (100.5 MHz, C_6D_6): δ 29.85 (t, J_{P-P} = 2.5 Hz), 35.54 (t, J_{P-P} = 5.1 Hz), 39.98 (t, J_{P-P} = 17.0 Hz), 108.84, 118.88, 139.28 (t, J_{P-P} = 7.4 Hz). Elemental analysis calculated (%) for **5** ($C_{24}H_{44}BClN_2NiP_2$): C, 54.64; H, 8.41; N, 5.31. Found: C, 54.63; H, 8.38; N, 5.33.

Synthesis of (^{tBu}PBP)NiOTf (6). To a THF solution (10 mL) of **5** (627.5 mg, 1.190 mmol) was added a THF solution (5 mL) of AgOTf (320.9 mg, 1.249 mmol) at RT. The mixture was stirred for 30 min. Solvents were removed under reduced pressure. The product was dissolved in benzene, and silver salts were removed by filtration through Celite. Lyophilization of the filtrate gave **6** as a yellow solid (759 mg, 99%). Yellow crystals of **6** were grown by slow concentration

of a pentane solution of **6** via vapor diffusion into hexamethyldisiloxane. ^{1}H NMR (400 MHz, C_6D_6): δ 1.20 (t, 36H, $^3J_{P-H}$ = 6.8 Hz), 3.32 (s, 4H), 6.77 (dd, 2H, J_{H-H} = 5.7 Hz, J_{H-H} = 3.1 Hz), 7.05 (dd, 2H, J_{H-H} = 5.7 Hz, J_{H-H} = 3.1 Hz). ^{31}P{^{1}H} NMR (161.8 MHz, C_6D_6): δ 83.6. ^{11}B{^{1}H} NMR (128.4 MHz, C_6D_6): δ 31.6. ^{19}F{^{1}H} NMR (376.2 MHz, C_6D_6): δ −76.7. ^{13}C{^{1}H} NMR (100.5 MHz, C_6D_6): δ 29.52 (t, J_{P-P} = 2.6 Hz), 34.97 (t, J_{P-P} = 4.8 Hz), 38.99 (t, J_{P-P} = 18.1 Hz), 108.86, 119.34, 138.51 (t, J_{P-P} = 6.8 Hz). Elemental analysis calculated (%) for **6** ($C_{25}H_{44}BF_3N_2NiO_3P_2S$): C, 46.83; H, 6.92; N, 4.37. Found: C, 46.66; H, 7.01; N, 4.36.

Synthesis of (^{tBu}PBP)NiH (7). To a toluene solution (5 mL) of **6** (326.6 mg, 0.509 mmol) was added a toluene solution (3 mL) of ^{i}Pr$_2$Mg (73.2 mg, 0.662 mmol) at −78 °C. The mixture was slowly warmed to RT over 1 h and stirred at RT for 12 h. Solvents were removed under vacuum. The resulting solid was triturated with pentane three times. The product was extracted into pentane (15 mL) and filtered through Celite. The resulting filtrate was concentrated to ~4 mL and allowed to stand at −30 °C for 24 h, affording yellow crystals of **3** (190 mg, 76%). ^{1}H NMR (400 MHz, C_6D_6): δ −1.69 (t, NiH, 1H, $^2J_{P-H}$ = 34.6 Hz), 1.27 (t, 36H, $^3J_{P-H}$ = 6.3 Hz), 3.80 (s, 4H), 7.05 (dd, 2H, J_{H-H} = 5.4 Hz, J_{H-H} = 2.7 Hz), 7.19 (dd, 2H, J_{H-H} = 5.4 Hz, J_{H-H} = 2.7 Hz). ^{31}P{^{1}H} NMR (161.8 MHz, C_6D_6): δ 122.5. ^{11}B{^{1}H} NMR (128.4 MHz, C_6D_6): δ 47.6. ^{13}C{^{1}H} NMR (100.5 MHz, C_6D_6): δ 29.96 (t, J_{P-P} = 3.1 Hz), 34.65 (t, J_{P-P} = 6.3 Hz), 42.07 (t, J_{P-P} = 16.6 Hz), 109.28, 118.39, 140.36 (t, J_{P-P} = 7.8 Hz). Elemental analysis calculated (%) for **7** ($C_{24}H_{45}BN_2NiP_2$): C, 58.46; H, 9.20; N, 5.68. Found (from two independently prepared samples): C, 57.91; H, 9.11; N, 5.37 and C, 57.98; H, 9.15; N, 5.43.

Synthesis of (^{tBu}PBP)NiOC(H)O (8). *Method A* (in situ generation): A J. Young NMR tube containing a C_6D_6 solution of **7** was subjected to one freeze−pump−thaw cycle and then backfilled with 1 atm CO$_2$. Quantitative formation of **8** was observed immediately by multinuclear NMR spectroscopies. *Method B*: To a flask containing **7** (90 mg, 0.183 mmol) was added 5 mL of benzene. The flask was subjected to one freeze−pump−thaw cycle and backfilled with 1 atm CO$_2$. Removal of solvents under reduced pressure gave **8** as a yellow solid (96 mg, 98%). Yellow crystals of **8** were obtained by slow concentration of a pentane solution of **8** under an atmosphere of N$_2$ at RT. ^{1}H NMR (400 MHz, C_6D_6): δ 1.30 (t, 36H, $^3J_{P-H}$ = 6.5 Hz), 3.50 (t, 4H, $^3J_{P-H}$ = 1.9 Hz), 6.88 (dd, 2H, J_{H-H} = 5.7 Hz, J_{H-H} = 3.3 Hz), 7.12 (dd, 2H, J_{H-H} = 5.7 Hz, J_{H-H} = 3.3 Hz), 9.11 (s, NiOC(H)O, 1H). ^{31}P{^{1}H} NMR (161.8 MHz, C_6D_6): δ 85.2. ^{11}B{^{1}H} NMR (128.4 MHz, C_6D_6): δ 35.7. ^{13}C{^{1}H} NMR (100.5 MHz, C_6D_6): δ 29.58 (t, J_{P-P} = 2.9 Hz), 35.16 (t, J_{P-P} = 5.0 Hz), 39.84 (t, J_{P-P} = 17.8 Hz), 108.67, 118.88, 139.26 (t, J_{P-P} = 7.5 Hz), 167.61. Elemental analysis calculated (%) for **8** ($C_{25}H_{45}BN_2Ni_2O_2P_2$): C, 55.91; H, 8.45; N, 5.22. Found: C, 55.89; H, 8.24; N, 5.22.

■ ASSOCIATED CONTENT

ⓢ Supporting Information

Spectroscopic characterizations, crystallographic analyses (CIF), kinetic details, and computational data. This material is available free of charge via the Internet at http://pubs.acs.org.

■ AUTHOR INFORMATION

Corresponding Author

jpeters@caltech.edu

Notes

The authors declare no competing financial interest.

■ ACKNOWLEDGMENTS

McCrory for insightful discussions on kinetics. We also thank Prof. Gerard Parkin for insightful discussions on bonding.

■ REFERENCES

(1) *The Handbook of Homogeneous Hydrogenation*; de Vries, J. G., Elsevier, C. J., Eds.; Wiley-VCH: Weinheim, Germany, 2007.

(2) *Catalysis without Precious Metals*; Bullock, R. M., Ed.; Wiley-VCH: Weinheim, Germany, 2010.

(3) Hartwig, J. F. *Organotransition Metal Chemistry: From Bonding to Catalysis*; University Science Books: Sausalito, CA, 2010.

(4) (a) Knijnenburg, Q.; Horton, A. D.; van der Heijden, H.; Kooistra, T. M.; Hetterscheid, D. G. H.; Smits, J. M. M.; de Bruin, B.; Budzelaar, P. H. M.; Gal, A. W. *J. Mol. Catal. A: Chem.* **2005**, *232*, 151−159. (b) Monfette, S.; Turner, Z. R.; Semproni, S. P.; Chirik, P. J. *J. Am. Chem. Soc.* **2012**, *134*, 4561−4564. (c) Zhang, G.; Scott, B. L.; Hanson, S. K. *Angew. Chem., Int. Ed.* **2012**, *51*, 12102−12106. (d) Lin, T.-P.; Peters, J. C. *J. Am. Chem. Soc.* **2013**, *135*, 15310−15313. (e) Yu, R. P.; Darmon, J. M.; Milsmann, C.; Margulieux, G. W.; Stieber, S. C. E.; DeBeer, S.; Chirik, P. J. *J. Am. Chem. Soc.* **2013**, *135*, 13168−13184. (f) Camacho-Bunquin, J.; Ferguson, M. J.; Stryker, J. M. *J. Am. Chem. Soc.* **2013**, *135*, 5537−5540. (g) Zhang, G.; Vasudevan, K. V.; Scott, B. L.; Hanson, S. K. *J. Am. Chem. Soc.* **2013**, *135*, 8668−8681. (h) Gärtner, D.; Welther, A.; Rad, B. R.; Wolf, R.; Jacobi von Wangelin, A. *Angew. Chem., Int. Ed.* **2014**, *53*, 3722−3726.

(5) (a) Angulo, I. M.; Kluwer, A. M.; Bouwman, E. *Chem. Commun.* **1998**, 2689−2690. (b) Angulo, I. M.; Bouwman, E. *J. Mol. Catal. A: Chem.* **2001**, *175*, 65−72. (c) Vasudevan, K. V.; Scott, B. L.; Hanson, S. K. *Eur. J. Inorg. Chem.* **2012**, 4898−4906. (d) Wu, J.; Faller, J. W.; Hazari, N.; Schmeier, T. J. *Organometallics* **2012**, *31*, 806−809. (e) Harman, W. H.; Peters, J. C. *J. Am. Chem. Soc.* **2012**, *134*, 5080−5082.

(6) (a) Ray, K.; Petrenko, T.; Wieghardt, K.; Neese, F. *Dalton Trans.* **2007**, 1552−1566. (b) Chirik, P. J. *Inorg. Chem.* **2011**, *50*, 9737−9740. (c) Luca, O. R.; Crabtree, R. H. *Chem. Soc. Rev.* **2013**, *42*, 1440−1459.

(7) (a) Daida, E. J.; Peters, J. C. *Inorg. Chem.* **2004**, *43*, 7474−7485. (b) Fong, H.; Moret, M.-E.; Lee, Y.; Peters, J. C. *Organometallics* **2013**, *32*, 3053−3062.

(8) (a) Bonanno, J. B.; Henry, T. P.; Wolczanski, P. T.; Pierpont, A. W.; Cundari, T. R. *Inorg. Chem.* **2007**, *46*, 1222−1232. (b) Alcaraz, G.; Helmstedt, U.; Clot, E.; Vendier, L.; Sabo-Etienne, S. *J. Am. Chem. Soc.* **2008**, *130*, 12878−12879. (c) Yang, J. Y.; Bullock, R. M.; Shaw, W. J.; Twamley, B.; Fraze, K.; DuBois, M. R.; DuBois, D. L. *J. Am. Chem. Soc.* **2009**, *131*, 5935−5945. (d) He, T.; Tsvetkov, N. P.; Andino, J. G.; Gao, X.; Fullmer, B. C.; Caulton, K. G. *J. Am. Chem. Soc.* **2009**, *132*, 910−911. (e) Miller, A. J. M.; Labinger, J. A.; Bercaw, J. E. *J. Am. Chem. Soc.* **2010**, *132*, 3301−3303. (f) Gunanathan, C.; Milstein, D. *Acc. Chem. Res.* **2011**, *44*, 588−602. (g) Wade, C. R.; Gabbaï, F. P. *Angew. Chem., Int. Ed.* **2011**, *50*, 7369−7372. (h) Tsoureas, N.; Kuo, Y.-Y.; Haddow, M. F.; Owen, G. R. *Chem. Commun.* **2011**, *47*, 484−486. (i) Lin, T.-P.; Gabbaï, F. P. *J. Am. Chem. Soc.* **2012**, *134*, 12230−12238. (j) Pan, B.; Bezpalko, M. W.; Foxman, B. M.; Thomas, C. M. *Dalton Trans.* **2012**, *41*, 9083−9090. (k) Podiyanachari, S. K.; Fröhlich, R.; Daniliuc, C. G.; Petersen, J. L.; Mück-Lichtenfeld, C.; Kehr, G.; Erker, G. *Angew. Chem., Int. Ed.* **2012**, *51*, 8830−8833. (l) Gutsulyak, D. V.; Piers, W. E.; Borau-Garcia, J.; Parvez, M. *J. Am. Chem. Soc.* **2013**, *135*, 11776−11779. (m) Boone, M. P.; Stephan, D. W. *J. Am. Chem. Soc.* **2013**, *135*, 8508−8511. (n) Gloaguen, Y.; Jacobs, W.; de Bruin, B.; Lutz, M.; van der Vlugt, J. I. *Inorg. Chem.* **2013**, *52*, 1682−1684. (o) Ostapowicz, T. G.; Merkens, C.; Hölscher, M.; Klankermayer, J.; Leitner, W. *J. Am. Chem. Soc.* **2013**, *135*, 2104−2107. (p) Sgro, M. J.; Stephan, D. W. *Chem. Commun.* **2013**, *49*, 2610−2612.

(9) Two plausible reaction pathways that were considered include (1) concerted σ-bond metathesis and (2) oxidative addition at the metal followed by hydride migration to boron. See refs 10a and 10b.

(10) (a) Zeng, G.; Sakaki, S. *Inorg. Chem.* **2013**, *52*, 2844−2853. (b) Harman, W. H.; Lin, T.-P.; Peters, J. C. *Angew. Chem., Int. Ed.* **2014**, *53*, 1081−1086.

(11) (a) Miyaura, N.; Suzuki, A. *Chem. Rev.* **1995**, *95*, 2457−2483. (b) Waltz, K. M.; Hartwig, J. F. *Science* **1997**, *277*, 211−213. (c) Irvine, G. J.; Lesley, M. J. G.; Marder, T. B.; Norman, N. C.; Rice, C. R.; Robins, E. G.; Roper, W. R.; Whittell, G. R.; Wright, L. J. *Chem. Rev.* **1998**, *98*, 2685−2722. (d) Braunschweig, H.; Colling, M. *Coord. Chem. Rev.* **2001**, *223*, 1−51. (e) Cho, J.-Y.; Tse, M. K.; Holmes, D.; Maleczka, R. E.; Smith, M. R. *Science* **2002**, *295*, 305−308. (f) Dang, L.; Lin, Z.; Marder, T. B. *Chem. Commun.* **2009**, 3987−3995.

(12) (a) Iverson, C. N.; Smith, M. R. *J. Am. Chem. Soc.* **1995**, *117*, 4403−4404. (b) Dai, C.; Stringer, G.; Marder, T. B.; Baker, R. T.; Scott, A. J.; Clegg, W.; Norman, N. C. *Can. J. Chem.* **1996**, *74*, 2026−2031. (c) Sakaki, S.; Kai, S.; Sugimoto, M. *Organometallics* **1999**, *18*, 4825−4837. (d) Zhu, J.; Lin, Z.; Marder, T. B. *Inorg. Chem.* **2005**, *44*, 9384−9390. (e) Braunschweig, H.; Brenner, P.; Müller, A.; Radacki, K.; Rais, D.; Uttinger, K. *Chem.—Eur. J.* **2007**, *13*, 7171−7176.

(13) van der Vlugt, J. I. *Angew. Chem., Int. Ed.* **2010**, *49*, 252−255.

(14) Segawa, Y.; Yamashita, M.; Nozaki, K. *Organometallics* **2009**, *28*, 6234−6242.

(15) Pandey, K. K. *Coord. Chem. Rev.* **2009**, *253*, 37−55.

(16) (a) Dapporto, P.; Midollini, S.; Sacconi, L. *Inorg. Chem.* **1975**, *14*, 1643−1650. (b) Fryzuk, M. D.; Ng, J. B.; Rettig, S. J.; Huffman, J. C.; Jonas, K. *Inorg. Chem.* **1991**, *30*, 2437−2441. (c) Kersten, J. L.; Rheingold, A. L.; Theopold, K. H.; Casey, C. P.; Widenhoefer, R. A.; Hop, C. E. C. A. *Angew. Chem., Int. Ed. Engl.* **1992**, *31*, 1341−1343.

(17) (a) Green, M. L. H. *J. Organomet. Chem.* **1995**, *500*, 127−148. (b) Green, J. C.; Green, M. L. H.; Parkin, G. *Chem. Commun.* **2012**, *48*, 11481−11503.

(18) Evans, D. F. *J. Chem. Soc.* **1959**, 2003−2005.

(19) Evans, R.; Deng, Z.; Rogerson, A. K.; McLachlan, A. S.; Richards, J. J.; Nilsson, M.; Morris, G. A. *Angew. Chem., Int. Ed.* **2013**, *52*, 3199−3202.

(20) Given the subtle differences that exist between these two molecules, an averaged value is adopted for the following discussion.

(21) Cordero, B.; Gomez, V.; Platero-Prats, A. E.; Reves, M.; Echeverria, J.; Cremades, E.; Barragan, F.; Alvarez, S. *Dalton Trans.* **2008**, 2832−2838.

(22) (a) Kahn, O. *Molecular Magnetism*; VCH: New York, 1993. (b) Green, M. T. *J. Am. Chem. Soc.* **1999**, *121*, 7939−7940.

(23) Marchand, A. P.; Marchand, N. W. *Tetrahedron Lett.* **1971**, *12*, 1365−1368.

(24) Luehring, P.; Schumpe, A. *J. Chem. Eng. Data* **1989**, *34*, 250−252.

(25) (a) Osborn, J. A.; Jardine, F. H.; Young, J. F.; Wilkinson, G. *J. Chem. Soc. A* **1966**, 1711−1732. (b) Sánchez-Delgado, R. A.; Rosales, M. *Coord. Chem. Rev.* **2000**, *196*, 249−280.

(26) Gómez-Gallego, M.; Sierra, M. A. *Chem. Rev.* **2011**, *111*, 4857−4963.

(27) (a) Jeske, G.; Lauke, H.; Mauermann, H.; Schumann, H.; Marks, T. J. *J. Am. Chem. Soc.* **1985**, *107*, 8111−8118. (b) Zuffa, J. L.; Blohm, M. L.; Gladfelter, W. L. *J. Am. Chem. Soc.* **1986**, *108*, 552−553.

(28) (a) Reed, S. A.; White, M. C. *J. Am. Chem. Soc.* **2008**, *130*, 3316−3318. (b) Powers, D. C.; Ritter, T. *Acc. Chem. Res.* **2012**, *45*, 840−850. (c) Pérez-Temprano, M. H.; Casares, J. A.; Espinet, P. *Chem.—Eur. J.* **2012**, *18*, 1864−1884. (d) Radlauer, M. R.; Day, M. W.; Agapie, T. *J. Am. Chem. Soc.* **2012**, *134*, 1478−1481. (e) Mazzacano, T. J.; Mankad, N. P. *J. Am. Chem. Soc.* **2013**, *135*, 17258−17261.

(29) Jones, R. A.; Norman, N. C.; Seeberger, M. H.; Atwood, J. L.; Hunter, W. E. *Organometallics* **1983**, *2*, 1629−1634.

(30) (a) Tanabe, M.; Yumoto, R.; Osakada, K. *Chem. Commun.* **2012**, *48*, 2125−2127. (b) Nova, A.; Suh, H.-W.; Schmeier, T. J.; Guard, L. M.; Eisenstein, O.; Hazari, N.; Maseras, F. *Angew. Chem., Int. Ed.* **2014**, *53*, 1103−1108.

(31) (a) Bach, I.; Goddard, R.; Kopiske, C.; Seevogel, K.; Pörschke, K.-R. *Organometallics* **1999**, *18*, 10−20. (b) Li, T.; García, J. J.; Brennessel, W. W.; Jones, W. D. *Organometallics* **2010**, *29*, 2430−2445.

(32) Adhikari, D.; Huffman, J. C.; Mindiola, D. J. *Chem. Commun.* **2007**, 4489−4491.

(33) Morris, R. H. *Coord. Chem. Rev.* **2008**, *252*, 2381−2394.

(34) (a) Gründemann, S.; Limbach, H.-H.; Buntkowsky, G.; Sabo-Etienne, S.; Chaudret, B. *J. Phys. Chem. A* **1999**, *103*, 4752−4754. (b) Gelabert, R.; Moreno, M.; Lluch, J. M.; Lledós, A.; Pons, V.; Heinekey, D. M. *J. Am. Chem. Soc.* **2004**, *126*, 8813−8822.

(35) Pfirrmann, S.; Yao, S.; Ziemer, B.; Stösser, R.; Driess, M.; Limberg, C. *Organometallics* **2009**, *28*, 6855−6860.

(36) Lill, S. O. N.; Siegbahn, P. E. M. *Biochemistry* **2009**, *48*, 1056−1066.

(37) Bader, R. F. W. *Atoms in Molecules: A Quantum Theory*; Oxford University Press: Oxford, U.K., 1994.

(38) (a) Barnett, B. L.; Krüger, C.; Tsay, Y.-H.; Summerville, R. H.; Hoffmann, R. *Chem. Ber.* **1977**, *110*, 3900−3909. (b) Fryzuk, M. D.; Clentsmith, G. K. B.; Leznoff, D. B.; Rettig, S. J.; Geib, S. J. *Inorg. Chim. Acta* **1997**, *265*, 169−177. (c) Cornella, J.; Gómez-Bengoa, E.; Martin, R. *J. Am. Chem. Soc.* **2013**, *135*, 1997−2009.

(39) Segawa, Y.; Yamashita, M.; Nozaki, K. *J. Am. Chem. Soc.* **2009**, *131*, 9201−9203.

(40) (a) Darensbourg, D. J.; Darensbourg, M. Y.; Goh, L. Y.; Ludvig, M.; Wiegreffe, P. *J. Am. Chem. Soc.* **1987**, *109*, 7539−7540. (b) Darensbourg, M. Y.; Ludwig, M.; Riordan, C. G. *Inorg. Chem.* **1989**, *28*, 1630−1634. (c) Chakraborty, S.; Zhang, J.; Krause, J. A.; Guan, H. *J. Am. Chem. Soc.* **2010**, *132*, 8872−8873. (d) Schmeier, T. J.; Hazari, N.; Incarvito, C. D.; Raskatov, J. A. *Chem. Commun.* **2011**, *47*, 1824−1826. (e) Suh, H.-W.; Schmeier, T. J.; Hazari, N.; Kemp, R. A.; Takase, M. K. *Organometallics* **2012**, *31*, 8225−8236. (f) Chakraborty, S.; Patel, Y. J.; Krause, J. A.; Guan, H. *Polyhedron* **2012**, *32*, 30−34. (g) Chakraborty, S.; Zhang, J.; Patel, Y. J.; Krause, J. A.; Guan, H. *Inorg. Chem.* **2013**, *52*, 37−47. (h) Venkanna, G. T.; Tammineni, S.; Arman, H. D.; Tonzetich, Z. J. *Organometallics* **2013**, *32*, 4656−4663.

(41) Gibson, D. H. *Coord. Chem. Rev.* **1999**, *185−186*, 335−355.

(42) (a) van der Vlugt, J. I.; Lutz, M.; Pidko, E. A.; Vogt, D.; Spek, A. L. *Dalton Trans.* **2009**, 1016−1023. (b) Vogt, M.; Rivada-Wheelaghan, O.; Iron, M. A.; Leitus, G.; Diskin-Posner, Y.; Shimon, L. J. W.; Ben-David, Y.; Milstein, D. *Organometallics* **2013**, *32*, 300−308.

(43) (a) Benito-Garagorri, D.; Bocokić, V.; Mereiter, K.; Kirchner, K. *Organometallics* **2006**, *25*, 3817−3823. (b) Gómez-Benítez, V.; Baldovino-Pantaleón, O.; Herrera-Álvarez, C.; Toscano, R. A.; Morales-Morales, D. *Tetrahedron Lett.* **2006**, *47*, 5059−5062. (c) Pandarus, V.; Zargarian, D. *Organometallics* **2007**, *26*, 4321−4334. (d) Boro, B. J.; Dickie, D. A.; Goldberg, K. I.; Kemp, R. A. *Acta Crystallogr., Sect. E* **2008**, *64*, m1304. (e) Chakraborty, S.; Krause, J. A.; Guan, H. *Organometallics* **2009**, *28*, 582−586. (f) Zhang, J.; Medley, C. M.; Krause, J. A.; Guan, H. *Organometallics* **2010**, *29*, 6393−6401. (g) Duncan, D.; Hope, E. G.; Singh, K.; Stuart, A. M. *Dalton Trans.* **2011**, *40*, 1998−2005.

(44) Castonguay, A.; Sui-Seng, C.; Zargarian, D.; Beauchamp, A. L. *Organometallics* **2006**, *25*, 602−608.

(45) Mitton, S. J.; McDonald, R.; Turculet, L. *Angew. Chem., Int. Ed.* **2009**, *48*, 8568−8571.

(46) (a) Liang, L.-C.; Chien, P.-S.; Lee, P.-Y. *Organometallics* **2008**, *27*, 3082−3093. (b) Boro, B. J.; Duesler, E. N.; Goldberg, K. I.; Kemp, R. A. *Inorg. Chem.* **2009**, *48*, 5081−5087. (c) Steinke, T.; Shaw, B. K.; Jong, H.; Patrick, B. O.; Fryzuk, M. D. *Organometallics* **2009**, *28*, 2830−2836. (d) Martínez-Prieto, L. M.; Melero, C.; del Río, D.; Palma, P.; Cámpora, J.; Álvarez, E. *Organometallics* **2012**, *31*, 1425−1438. (e) Sgro, M. J.; Stephan, D. W. *Organometallics* **2012**, *31*, 1584−1587.

(47) Keim, W. *Angew. Chem., Int. Ed. Engl.* **1990**, *29*, 235−244.

(48) (a) Threlkel, R. S.; Bercaw, J. E. *J. Am. Chem. Soc.* **1981**, *103*, 2650−2659. (b) Parkin, G.; Bunel, E.; Burger, B. J.; Trimmer, M. S.; Van Asselt, A.; Bercaw, J. E. *J. Mol. Catal.* **1987**, *41*, 21−39. (c) Cheng, T.-Y.; Bullock, R. M. *J. Am. Chem. Soc.* **1999**, *121*, 3150−3155. (d) Jones, W. D. *Acc. Chem. Res.* **2003**, *36*, 140−146.

(49) Bullock, R. M.; Samsel, E. G. *J. Am. Chem. Soc.* **1990**, *112*, 6886−6898.

(50) A similar mechanism has been proposed for the catalyst (^{Cy}PNHP)NiH^+ by Hanson. See ref 5c.

(51) Böhm, V. P. W.; Schulze, V.; Brönstrup, M.; Müller, M.; Hoffmann, R. W. *Organometallics* **2003**, *22*, 2925−2930.

(52) Sheldrick, G. M. *SADABS*, version 2007/4; Bruker Analytical X-ray Systems: Madison, WI, 2007.

(53) Sheldrick, G. M.; *SHELXTL*, version 6.1; Bruker Analytical X-ray Systems: Madison, WI, 2000.

(54) Frisch, M. J.; Trucks, G. W.; Schlegel, H. B.; Scuseria, G. E.; Robb, M. A.; Cheeseman, J. R.; Montgomery, J. A., Jr.; Vreven, T.; Kudin, K. N.; Burant, J. C.; Millam, J. M.; Iyengar, S. S.; Tomasi, J.; Barone, V.; Mennucci, B.; Cossi, M.; Scalmani, G.; Rega, N.; Petersson, G. A.; Nakatsuji, H.; Hada, M.; Ehara, M.; Toyota, K.; Fukuda, R.; Hasegawa, J.; Ishida, M.; Nakajima, T.; Honda, Y.; Kitao, O.; Nakai, H.; Klene, M.; Li, X.; Knox, J. E.; Hratchian, H. P.; Cross, J. B.; Bakken, V.; Adamo, C.; Jaramillo, J.; Gomperts, R.; Stratmann, R. E.; Yazyev, O.; Austin, A. J.; Cammi, R.; Pomelli, C.; Ochterski, J. W.; Ayala, P. Y.; Morokuma, K.; Voth, G. A.; Salvador, P.; Dannenberg, J. J.; Zakrzewski, V. G.; Dapprich, S.; Daniels, A. D.; Strain, M. C.; Farkas, O.; Malick, D. K.; Rabuck, A. D.; Raghavachari, K.; Foresman, J. B.; Ortiz, J. V.; Cui, Q.; Baboul, A. G.; Clifford, S.; Cioslowski, J.; Stefanov, B. B.; Liu, G.; Liashenko, A.; Piskorz, P.; Komaromi, I.; Martin, R. L.; Fox, D. J.; Keith, T.; Al-Laham, M. A.; Peng, C. Y.; Nanayakkara, A.; Challacombe, M.; Gill, P. M. W.; Johnson, B.; Chen, W.; Wong, M. W.; Gonzalez, C.; Pople, J. A. *Gaussian 03*, revision C.02; Gaussian, Inc.: Wallingford, CT, 2004.

(55) (a) Perdew, J. P. *Phys. Rev. B* **1986**, *33*, 8822−8824. (b) Becke, A. D. *Phys. Rev. A* **1988**, *38*, 3098−3100.

(56) (a) Hall, M. B.; Fenske, R. F. *Inorg. Chem.* **1972**, *11*, 768−775. (b) Manson, J.; Webster, C. E.; Pérez, L. M.; Hall, M. B. http://www.chem.tamu.edu/jimp2/index.html.

(57) Konig, F. B.; Schonbohm, J.; Bayles, D. *J. Comput. Chem.* **2001**, *22*, 545−559.

13683

dx.doi.org/10.1021/ja504667f | *J. Am. Chem. Soc.* 2014, 136, 13672−13683